Infection and Drug Resistance

Dovepress
open access to scientific and medical research

Open Access Full Text Article

ORIGINAL RESEARCH

Evaluation of the Effect and Mechanism of Sanhuang Ointment on MRSA Infection in the Skin and Soft Tissue via Network Pharmacology

Haibang Pan[1,*], Tianming Wang[1,2,*], Ying Che[3,4], Xiaoli Li[1,5], Yan Cui[1], Quanxin Chen[1], Zhihang Wu[1], Jianfeng Yi[1], Bo Wang[3]

[1]First School of Clinical Medicine, Gansu University of Chinese Medicine, Lanzhou, People's Republic of China; [2]Gansu Provincial Key Laboratory of Traditional Chinese Medicine Recipe Mining and Innovation Transformation, Gansu Province New Production of Traditional Chinese Medicine Product Creation Engineering Laboratory, Lanzhou, People's Republic of China; [3]School of Nursing, Gansu University of Chinese Medicine, Lanzhou, People's Republic of China; [4]Research Ward, Gansu Provincial People's Hospital, Lanzhou, People's Republic of China; [5]Gansu Provincial Maternity and Child-Care Hospital, Lanzhou, People's Republic of China

*These authors contributed equally to this work

Correspondence: Bo Wang; Jianfeng Yi, Email wbbphb@gszy.edu.cn; yijf02@163.com

Introduction: Skin and soft tissue infection (SSTI) is a frequently encountered clinical disease, and Sanhuang ointment, a traditional Chinese medicine, is used to treat it. However, the pharmacological effect of Sanhuang ointment on SSTI and its underlying mechanism remains unclear. Here, we investigate the protective effect of Sanhuang ointment on *Methicillin-resistant Staphylococcus aureus* (MRSA) infection in the skin and soft tissues and the underlying mechanism by network pharmacological analysis, followed by in vivo experimental validation.

Methods: Via network pharmacology, the active components and disease targets of Sanhuang ointment were screened and intersected for Gene Ontology (GO) and Kyoto Encyclopedia of Genes and Genomes (KEGG) enrichment analysis. A rat model of skin and soft tissue infection was established, and pathological features were observed. Large, medium, and small-dose groups (1 g, 0.5 g, and 0.25 g/animal, with the total amount of Vaseline, dispensed 1 g/animal) of Sanhuang ointment were prepared and Mupirocin ointment was used as a positive control (0.5 g/animal, with the total amount of Vaseline, dispensed 1 g/animal). The expressions of key proteins of the IL-17/NF-κB signaling pathway and downstream inflammatory factors were analyzed by histomorphological analysis, enzyme-linked immunosorbent assay, polymerase chain reaction, and Western blotting.

Results: In all, 119 active components and 275 target genes of Sanhuang ointment were identified and intersected with MRSA infection-related genes via network pharmacology analysis, and 34 target genes of Sanhuang ointment were found to be involved in skin and soft tissue infections with MRSA. Sanhuang ointment (1 g/mouse) could effectively ameliorate histopathological changes and significantly inhibit the expression of key proteins involved in the IL-17/NF-κB signaling pathway and downstream inflammatory factors ($p < 0.05$).

Conclusion: Sanhuang ointment has a protective effect on MRSA infection and inhibits inflammation by inhibiting the IL-17/NF-κB signaling pathway. Our findings are important for the secondary development and new drug development of Sanhuang ointment.

Plain Language Summary: Sanhuang ointment can significantly inhibit inflammatory response after skin and soft tissue infection with MRSA.

Sanhuang ointment may inhibit the inflammatory response induced by MRSA in the skin and soft tissue infections by targeting the IL-17/NF-κB signaling pathway.

We study the active components and mechanism of action of Sanhuang ointment on MRSA infection through network pharmacology.

Keywords: Sanhuang ointment, MRSA, SSTI, network pharmacology, IL-17, NF-κB

Received: 7 June 2023
Accepted: 27 October 2023
Published: 7 November 2023

Introduction

Skin and soft tissue infections (SSTIs) are common clinical diseases.[1] Most soft tissue infections are inflammatory reactions mainly caused by pathogenic invasion and reproduction. Bacterial infections (most commonly caused by *Staphylococcus aureus* and *Hemolytic Streptococci*) are common problems faced while treating soft tissue infections on the body surface.[2] *Methicillin-resistant Staphylococcus aureus* (MRSA) is the most commonly encountered drug-resistant *Staphylococcus aureus*, with increasing detection rates in body surface-infected tissues, secretions, and pus. MRSA has become bacteria with the highest incidence of nosocomial infections worldwide.[3] According to the Global Surveillance System for Antibiotic Resistance and Use (GLASS) report survey statistics in 2020, approximately 700,000 deaths resulting from antibiotic-resistant bacterial infections are reported each year worldwide, and MRSA is one of its major risk factors.[4] At present, vancomycin is the first-line antibiotic used for the clinical treatment of MRSA infections, but the increasing number of vancomycin-resistant strains has increased the complexity of clinical anti-MRSA infection treatment[5,6] Although some progress has been made in the research and development of new antibiotics for treating MRSA infections in recent years, it is important to find new treatment strategies to prevent the emergence of new antibiotic-resistant strains.

"Sanhuang ointment" (in-hospital preparation of the Affiliated Hospital of Gansu University of Traditional Chinese Medicine, Ganyao Zhunzi Z04010878). Huangqin, Huanglian, Huangbai, Borneol, sesame oil, and Vaseline, among others are prepared in specific proportions. Huangqin, the dried rhizome of *Scutellariae Radix*. Huanglian, the dried rhizome of *Coptidis Rhizoma*. Huangbai, the dried rhizome of *Phellodendri Chinensis Cortex*. The plant name corresponds to the latest revision in "World Flora Online" (www.worldfloraonline.org). It has been clinically used for more than 35 years, with significant curative effects and few side effects, especially for boils, carbuncles, erysipelas, abscesses, and other acute and chronic purulent infections, burns, soft tissue injuries, fluid extravasation, body surface ulcers, banding caused by infusion and chemotherapy, Herpes and other infectious diseases and has a significant curative effect.[7–9] Chemical analysis of Sanhuang ointment by ultra-performance liquid chromatography-mass spectrometry (UPLCQ-MS/MS) found that the main components of Coptidis Rhizoma were alkaloids, among which magnolia, berberine, coptisine, jatrorrhizine, palmatine, and Berberine inhibit *Staphylococcus aureus*.[10] The main components of Phellodendri Chinensis Cortex are alkaloids (such as berberine, palmatine, and Phellodendron), which are known as anti-inflammatory agents,[11,12] and work by inhibiting nuclear factor (NF) activation of kappa-B (κB) and mitogen-activated protein kinase (MAPK) and downregulation of nitrogen monoxide (NO) and inducible nitric oxide synthase (iNOS) for anti-inflammatory purposes.[13] The main active components of Scutellariae Radix are flavonoids such as baicalin, baicalein, wogonin, and oroxylin A.[14–16] Antioxidant and anti-inflammatory effects have been demonstrated in various disease models, including diabetes, cardiovascular disease, inflammatory bowel disease, gout, rheumatoid arthritis, asthma, neurodegenerative diseases, liver and kidney disease, cerebrospinal inflammation, and cancer.[17] Previous studies have found that Sanhuang ointment can treat the inflammatory response caused by *methicillin-resistant Staphylococcus aureus* infection in rat subcutaneous soft tissue by inhibiting the key proteins of the TLR2/NF-κB signaling pathway and its downstream inflammatory factors.[18]

Network pharmacology is an emerging pharmacological research field integrating traditional pharmacology, bioinformatics, chemoinformatics, and network biology,[19,20] and it can systematically determine the active ingredients and potential mechanisms of action of traditional Chinese medicines.[21,22] We used network pharmacology to predict whether Sanhuang ointment treats skin and soft tissue infections caused by MRSA via the IL-17/NF-κB signaling pathway. A rat model of skin and soft tissue infection caused by MRSA was developed by a subcutaneous injection of MRSA bacterial suspension. After intervention with Sanhuang ointment, histopathological analysis was performed to determine the chances of infection. The expression levels of IL-17, TRAF6, TAK1, TAB1, IKKβ, NF-κB p65, and inflammatory cytokines IL-1β, IL-4, IL-5, IL-6, TNF-α, and IFN-γ, which are key proteins in the IL-17/NF-κB signaling pathway, were also determined, thus confirming the role of Sanhuang ointment in the treatment of MRSA infection on the skin and soft tissue and the involvement of IL-17/NF-κB signaling pathway.

Materials and Methods

Preparation of Sanhuang Ointment and Collection, Screening, and Target Prediction of Chemical Constituents

Sanhuang ointment is composed of Coptidis Rhizoma, Scutellariae Radix, and Phellodendri Chinensis Cortex, according to the Chinese Pharmacopoeia 2020 edition. All medicinal materials were purchased from Lanzhou Foci Pharmaceutical Industry Development Group Co., Ltd. These medicinal materials were identified by Professor Guotai Wu of Gansu University of Traditional Chinese Medicine and stored in the pharmacy of the Affiliated Hospital of Gansu University of Traditional Chinese Medicine. Preparation of Sanhuang plaster powder: 60 g of Coptidis Rhizoma, 30 g of Phellodendri Chinensis Cortex, and 30 g of Scutellariae Radix were washed with water and dried. The aforementioned drugs were then mixed, crushed, passed through a 100-mesh sieve, dispensed, and sterilized. Preparation of Sanhuang ointment: 36 g sesame oil was placed in a stainless steel pot and brought to a boil; 36 g petrolatum was added, and after melting, Sanhuang ointment powder was added and mixed thoroughly by stirring until completely solidified. Dispense, then.

Upon referring to the Systematic Pharmacology Database of Traditional Chinese Medicine (TCMSP, https://tcmspw.com/TCMSP.php),[23] the active ingredients of Sanhuang ointment were predicted. Ingredients from Sanhuang ointment were filtered by drug-likeness (DL). DL is a qualitative concept used in drug design for an estimate on how "drug-like" a prospective compound is. This vital property is used as a selection criterion for the "drug-like" compounds in the traditional Chinese herbs and it helps to optimize pharmacokinetic and pharmaceutical properties. A drug similarity (DL) of ≥0.18 with the screening threshold was indicative of the active ingredient of Sanhuang ointment. Finally, all target names were converted into standard gene symbols using the UniProt database (https://www.UniProt.org/).[24] Because Sanhuang ointment is a topical formulation, its first-pass effect is not related to liver and kidney metabolism, but it rather acts directly on the target organs. Accordingly, oral bioavailability cannot be used for screening.

MRSA Infection Target Search

The keyword "methicillin-resistant Staphylococcus aureus infection" was used to screen for relevant targets in the Gene Cards database (https://www.genecards.org/), Drug Bank database (https://go.drugbank.com/), TTD database (https://db.idrblab.net/ttd/), the DisGeNET database (https://www.disgenet.org/), and the OMIM database (https://omim.org/),[25] removing duplicate values after retrieval.

Network Construction and Analysis

The active ingredient of Sanhuang ointment and the corresponding targets were introduced into Cytoscape 3.7.2 (https://Cytoscape.org/index.html) software to construct an "active component-target" network diagram. Subsequently, using the Venny platform (https://bioinfogp.cnb.csic.es/tools/venny/index.html), the target genes of Sanhuang ointment and the disease intersected. The intersected genes were selected as potential targets for Sanhuang ointment intervention during MRSA infection.

Construction and Analysis of Interaction Network

After introducing Sanhuang ointment and common targets of the disease into the STRING[26] database (https://string-db.org/cgi/input.pl), the protein interaction network was constructed. The species was selected as "Homo sapiens" with a minimum interaction score set as "0.900" and PPI network maps were exported after hiding free points. The active ingredients and corresponding targets of Sanhuang ointment were imported into Cytoscape 3.7.2 to construct the "active component-target" network diagram.

Gene Ontology (GO) and Kyoto Encyclopedia of Genes and Genomes (KEGG) Pathway Enrichment Analysis

Based on the Sanhuang ointment target gene set and the *methicillin-resistant Staphylococcus aureus* infection-related gene set, a compound-target network is constructed by means of Cytoscape version 3.8.0. Enrichment analysis, including gene ontology (GO) and Kyoto Encyclopedia of Genes and Genomes (KEGG) pathway analysis, was performed to reveal

the underlying mechanism through biological processes, cellular components, molecular function, and key signalling pathways.

Phytochemical Analysis of Sanhuang Ointment

Sample Preparation and Extraction

For sample preparation, 50 mg of the mixed sample was taken and placed in a 2 mL Eppendorf tube. Subsequently, 1200 μL 70% methanol internal standard extract solution was added and Vortexed for 15 min. This was followed by centrifugation (12,000 r/min, 4°C) for 10 min; the supernatant was filtered with a microporous filter membrane (0.22 μm) and stored in an injection bottle for liquid chromatography-tandem mass spectrometry (LC-MS/MS) test.

UPLC Conditions

The sample extracts were analyzed using a rapid and sensitive ultra-performance liquid chromatography electrospray ionization mass spectrometry (UPLC-ESI-MS/MS) system (UPLC, ExionLC™ AD, https://sciex.com.cn/; MS, Applied Biosystems 6500 Q TRAP, https://sciex.com.cn/). The analysis conditions were as follows: UPLC column, Agilent SB-C18 (1.8 μm, 2.1 mm * 100 mm); the mobile phase comprised solvent A, pure water with 0.1% formic acid, and solvent B, acetonitrile with 0.1% formic acid. Sample measurements were performed with a gradient program employing the starting conditions of 95% A, 5% B. Within 9 min, a linear gradient to 5% A, 95% B was programmed, and the composition of 5% A, 95% B was maintained for 1 min. Subsequently, a composition of 95% A, 5% B was adjusted within 1.1 min and maintained for 2.9 min. The flow velocity was set to 0.35 mL per minute. The column oven was set to 40°C, and the injection volume was 2 μL. The effluent was alternatively connected to an ESI-triple quadrupole-linear ion trap (Q TRAP)-MS.

Triple Quadrupole-Linear Ion Trap Mass Spectrometer

The ESI source operation parameters were as follows: source temperature 500°C; ion spray voltage (IS) 5500 V (positive ion mode)/-4500 V (negative ion mode); ion source gas I (GSI), gas II (GSII), and curtain gas (CUR) were set at 50, 60, and 25 psi, respectively; the collision-activated dissociation (CAD) was high. QQQ scans were acquired as multiple reaction monitoring (MRM) experiments with collision gas (nitrogen) set to medium. The declustering potential (DP) and collision energy (CE) for individual MRM transitions were evaluated with further DP and CE optimization. A specific set of MRM transitions was monitored for each period according to the metabolites eluted within the period.

Experimental Animals

In all, 96 Specific pathogen Free (SPF) healthy Wistar rats, in 1:1 male:female ratio, weighing 280 ± 10 g, were provided by the Medical Experimental Center of Gansu University of Traditional Chinese Medicine with animal license number SCXK (Gan) 2015-0002. The rats were housed in the SPF laboratory of the Scientific Research Experimental Center, Gansu University of Traditional Chinese Medicine. Experimental animals were handled keeping in mind all animal ethical principles. The study was approved by Ethics Committee of Institutional Committee for the Protection and Use of Animals at Gansu University of Chinese Medicine (2022–545), and all experiments were conducted in accordance with the relevant guidelines and regulations. This study was performed in compliance with the ARRIVE guidelines. All animal experiments were carried out in accordance with the EU Directive 2010/63/EU. All ARRIVE guidelines were adhered to, and the checklist was supplied.

Main Reagents

The following reagents were used in the study: Sanhuang Ointment, provided by Affiliated Hospital of Gansu University of Traditional Chinese Medicine, batch number (210329); Mupirocin Ointment, Sino-American Tianjin Shi Ke Pharmaceutical Co., Ltd., batch number 3L4K; MRSA (ATCC 25923), gifted by Clinical Medical Translation Center of Gansu Provincial People's Hospital; IL-4, IL-5, IL-17, TNF-α, IL-1β, IL-6, and IFN-γ ELISA kits (article numbers JL13252, JL13268, JL13282, JL13202, JL20884, JL20897, and JL207308, respectively, Shanghai Future Industrial Co., Ltd.; TRAF6, TAK1, TAB1, IKKβ, and NF-κB p65 antibodies (batch numbers GR3277367-3, GR190324-31,

GR3273233-1, GR117080-30, and GR32932611, respectively), GeneTex, USA; TRlzol (batch No. 152104), Ambion, USA; reverse transcription kit and RT-qPCR kit (batch numbers AI40704A and AI61180A, respectively), TaKaRa, Japan; and GAPDH antibody (batch No. B1501), ImmunoWay, USA.

Animal Grouping, Model Making, and Intervention

The 96 Wistar rats were divided into blank, model, Mupirocin Ointment, and Sanhuang ointment high-, medium-, and low-dose groups according to a random number table after 1 week of adaptive feeding, with 16 rats in each group. According to the method designed by Malachowa et al[27] each rat was depilated in a 2×2 cm area marked with a signature pen near the cervical side of the back, considering the spine as the midline. The blank group did not receive any treatment, and the other groups of rats were subcutaneously injected with 1 mL MRSA suspension at a concentration of 6×10^8 CFU/mL, with purulent infection foci in the depilated area indicating successful modeling. On the day after model establishment, the external application was initiated. Mupirocin ointment was applied at a strength of 0.5 g/mouse in the Mupirocin ointment group (the total amount of ointment adjusted with Vaseline was 1 g/mouse). Further, the concentrations in the Sanhuang ointment high-, medium-, and low-dose groups were 1, 0.5, and 0.25 g/mouse, respectively (the total amount of ointment adjusted with Vaseline was 1 g/mouse), and the same amount of Vaseline was applied twice daily for 7 days in the blank and model groups. The general condition and soft tissue infection in rats were observed daily. Changes in skin tissue before and after modeling are shown in Figure 1.

Animal Handling and Tissue Collection

After 7 days of drug intervention in each observation group, 3% sodium pentobarbital was injected intraperitoneally (1mL/1000 g) to anesthetize the rats. 10–15 mL of whole blood was collected from the abdominal aorta, and finally the rats were killed by cervical dislocation. The surface infected tissues were separated, and some infected soft tissues were subjected to pathological detection; some tissues were routinely homogenized and ELISA was used to detect cytokine content. The other two parts of tissue were rinsed with ice-cold 0.9% sodium chloride, placed in cryopreservation tubes, and immediately placed in liquid nitrogen for storage. Real-time fluorescent quantitative PCR and immunohistochemistry were used to detect infected tissues on the surface of each group.

Hematoxylin-Eosin (HE) Staining for the Histopathological Detection of the Infection

Infected tissues were stained via HE staining. The procedure involved the following steps: the tissues were fixed in 4% paraformaldehyde, embedded in paraffin, sectioned, deparaffinized in xylene, dehydrated in graded ethanol, stained with hematoxylin, differentiated in hydrochloric acid in alcohol, dehydrated in graded ethanol, stained with eosin, cleared in xylene, mounted in neutral gum, and observed under a light microscope.

Detection of Infected Tissue and Serum by Enzyme-Linked Immunosorbent Assay

According to the instructions mentioned in the Enzyme-linked Immunosorbent Assay kit, the absorbance at 450 nm was measured using a microplate reader. The standard curve was drawn, and the contents of IL-1β, IL-4, IL-5, IL-6, IL-17, TNF-α, and IFN-γ in the serum and infected tissue samples were calculated.

Figure 1 Images comparing the skin tissue before and after modeling.

Detection of IL-1β, IL-4, IL-5, IL-6, IL-17, TNF-α, TRAF6, TAK1, TAB1, IKKβ, and NF-κB p65 mRNA Levels in the Serum and Infected Tissues by qRT-PCR

Total RNA from infected tissues was extracted by the Trizol method.[28] The cDNA was synthesized by reverse transcription using RNA as a template, and the reaction system and parameters were set according to the qRT-PCR kit instructions for PCR. The relative mRNA expression was calculated by the $2^{-\Delta\Delta Ct}$ method using β-actin as an internal reference. Primers were synthesized by Bao Biological Engineering (Dalian) Co., Ltd. The primer sequences are shown in Table 1.

Detection of TRAF6, TAK1, TAB1, IKKβ, and NF-κB p65 Protein Expression in the Infected Tissue by Immunocytochemistry

Infected paraffin sections were placed in a constant temperature oven at 72°C for 1 h and then placed in a machine for deparaffinization. Antigen retrieval and blocking sections were placed in a citrate buffer at pH 6.0 and then placed in a microwave oven for antigen retrieval. Antibody incubation decant the blocking solution on the sections, and approximately 80 μL of corresponding primary antibodies were added (TRAF6, TAK1, TAB1, IKKβ, and NF-κB p65) dropwise to each section. PBS was discarded, and 80 μL of secondary antibody conjugated with horseradish peroxidase (HRP) was added dropwise, followed by incubation at room temperature for 30 min. A fresh DAB chromogenic solution (850 μL deionized water + 150 μL working solution) was prepared. The slide was placed under the microscope while developing the color, and approximately 60 μL of color developing solution was added dropwise. The color change was observed under a light microscope, and the reaction time was controlled depending on the color change. The sections were immediately placed in tap water to terminate the reaction. All sections were rinsed with tap water for 10 min after color development and then counterstained in hematoxylin for 10–20 s (staining time was determined according to the freshness of the hematoxylin preparation, and overstaining was not allowed). After counterstaining, the sections were quickly placed in tap water to terminate the reaction, and rinsed for 10 min. The sections were allowed to naturally dry, and a drop of 10% neutral gum was added dropwise to cover the slides.

Table 1 PCR Primer Sequences of Each Gene

Gene Name	Primer Sequences (5'~3')	Length of Output/bp
β-actin	F: GGAGATTACTGCCCTGGCTCCTA R: GACTCATCGTACTCCTGCTTGCTG	102
IL-1β	F: CCTGAACTCAACTGTGAAATAGCA R:CCCAAGTCAAGGGCTTGGAA	123
IL-4	F: TGCACCGAGATGTTTGTACCAGA R:TTGCGAAGCACCCTGGAAG	92
IL-5	F: CCTTGATACAGCTGTCCACTCAC R: CCCTCGGACAGTTTGATTCTT	146
IL-6	F: TTGTATGAACAGCGATGATGCAC R:CCAGGTAGAAACGGAACTCCAGA	150
IL-17	F: AGCGTGTCCAAACACTGAGG R:ACGTGGAACGGTTGAGGTAG	125
TNF-α	F: TTCCAATGGGCTTTCGGAAC R: AGACATCTTCAGCAGCCTTGTGAG	118
TRAF6	F: CAGTGGTCGTATCGTGCTTA R:CCTTATGGTTTCTTGGAGTC	120
TAK1	F: TATGCTGAAGGAGGCTCGTTGT R:AGGCTTGAGGTCCCTATGAATG	162
TAB1	F: CTGGAGAGCTTGGAGGACGA R:TCGCAAGAACCAGAATAAGAAGTG	159
IKKβ	F: GCACCCTGGCCTTTGAATG R: TCCGTTCAAGTCCTCGCTAACA	128
NF-κB p65	F: TCTTCGACTACGCGGTTACGG R:CTCACGAGCTGAGCATGAAGG	133

Statistical Analysis

Comparison analysis was performed via a one-way analysis of variance (ANOVA) using GraphPad Prism 9 software to compare differences between groups and to compare the least significant difference (LSD). Significant difference was indicated by $\alpha = 0.05$ and $p < 0.05$ at the two-sided test levels.

Results

Construction and Analysis of the "Active Ingredient-Target" Network of Sanhuang Ointment

In TCMSP, a total of 151 effective active compounds of Sanhuang ointment were screened based on DL, including 72 kinds of Scutellariae Radix, 31 kinds of Coptidis Rhizoma, and 70 kinds of Phellodendri Chinensis Cortex (compound details are shown in Table 2). Among them, Coptidis Rhizoma, Phellodendri Chinensis Cortex, and Scutellaria Radix share components of jatrorrhizine and coptisine. Coptidis Rhizoma and Phellodendri Chinensis Cortex share the ingredients berberine, columbamine, magnoflorine, berberrubine, phellodendrine, magnograndiolide, palmatine, quercetin, and Worenine. The common component of Coptidis Rhizoma and Scutellariae Radix is epiberberine; Phellodendri Chinensis Cortex and Scutellariae Radix common components are Sitogluside, beta-sitosterol, and Stigmasterol. The targets of effective active compounds were searched in the TCMSP database, and after removing duplicate data, 275 targets related to components were obtained. The active ingredients and corresponding targets of Sanhuang ointment were imported into Cytoscape 3.7.2 software to construct the "active component-

Table 2 Main Chemical Constituents of Sanhuang Ointment

NO.	Mol ID	Component Name	DL	Herb
1	MOL001689	Acacetin	0.24	Scutellariae Radix
2	MOL000173	Wogonin	0.23	Scutellariae Radix
3	MOL013068	Oroxindin	0.77	Scutellariae Radix
4	MOL000228	(2R)-7-hydroxy-5-methoxy-2-phenylchroman-4-one	0.2	Scutellariae Radix
5	MOL002560	Chrysin	0.18	Scutellariae Radix
6	MOL002714	Baicalein	0.21	Scutellariae Radix
7	MOL002737	Scutellarein	0.24	Scutellariae Radix
8	MOL002908	5,8,2'-Trihydroxy-7-methoxyflavone	0.27	Scutellariae Radix
9	MOL002909	5,7,2,5-tetrahydroxy-8,6-dimethoxyflavone	0.45	Scutellariae Radix
10	MOL002910	Carthamidin	0.24	Scutellariae Radix
11	MOL002911	2,6,2',4'-tetrahydroxy-6'-methoxychaleone	0.22	Scutellariae Radix
12	MOL002912	Dihydrobaicalin	0.75	Scutellariae Radix
13	MOL002913	Dihydrobaicalin_qt	0.21	Scutellariae Radix
14	MOL002914	Eriodyctiol (flavanone)	0.24	Scutellariae Radix
15	MOL002915	Salvigenin	0.33	Scutellariae Radix
16	MOL002916	2-(2,6-dihydroxyphenyl)-3,5,7-trihydroxy-chromone	0.27	Scutellariae Radix
17	MOL002917	5,2',6'-Trihydroxy-7,8-dimethoxyflavone	0.33	Scutellariae Radix
18	MOL002918	Ganhuangenin	0.37	Scutellariae Radix
19	MOL002919	Viscidulin III	0.37	Scutellariae Radix
20	MOL002921	(2S,3R,4R,5R,6S)-2-[(2R,3R,4S,5R,6R)-3,5-dihydroxy-2-[2-(3-hydroxy-4-methoxy-phenyl)ethoxy]-6-methylol-tetrahydropyran-4-yl]oxy-6-methyl-tetrahydropyran-3,4,5-triol	0.67	Scutellariae Radix
21	MOL002923	Darendoside B	0.59	Scutellariae Radix
22	MOL002924	Darendoside B_qt	0.22	Scutellariae Radix
23	MOL002925	5,7,2',6'-Tetrahydroxyflavone	0.24	Scutellariae Radix
24	MOL002926	Dihydrooroxylin A	0.23	Scutellariae Radix
25	MOL002927	Skullcapflavone II	0.44	Scutellariae Radix
26	MOL002928	Oroxylin a	0.23	Scutellariae Radix
27	MOL002929	Salidroside	0.2	Scutellariae Radix
28	MOL002931	Scutellarin	0.79	Scutellariae Radix

(*Continued*)

Table 2 (Continued).

NO.	Mol ID	Component Name	DL	Herb
29	MOL002932	Panicolin	0.29	Scutellariae Radix
30	MOL002933	5,7,4'-Trihydroxy-8-methoxyflavone	0.27	Scutellariae Radix
31	MOL002934	NEOBAICALEIN	0.44	Scutellariae Radix
32	MOL002935	Baicalin	0.77	Scutellariae Radix
33	MOL002936	5,8-Dihydroxy-6,7-dimethoxyflavone	0.29	Scutellariae Radix
34	MOL002937	DIHYDROOROXYLIN	0.23	Scutellariae Radix
35	MOL000359	Sitosterol	0.75	Scutellariae Radix
36	MOL000396	(+)-Syringaresinol	0.72	Scutellariae Radix
37	MOL000458	Campesterol	0.72	Scutellariae Radix
38	MOL000525	Norwogonin	0.21	Scutellariae Radix
39	MOL000552	5,2'-Dihydroxy-6,7,8-trimethoxyflavone	0.35	Scutellariae Radix
40	MOL000007	Cosmetin	0.74	Scutellariae Radix
41	MOL000008	Apigenin	0.21	Scutellariae Radix
42	MOL000073	Ent-Epicatechin	0.24	Scutellariae Radix
43	MOL000654	Methyl montanate	0.48	Scutellariae Radix
44	MOL000870	HEXATRIACONTANE	0.41	Scutellariae Radix
45	MOL001490	bis[(2S)-2-ethylhexyl] benzene-1,2-dicarboxylate	0.35	Scutellariae Radix
46	MOL001506	Supraene	0.42	Scutellariae Radix
47	MOL002027	Methyl behenate	0.29	Scutellariae Radix
48	MOL002819	Catalpol	0.44	Scutellariae Radix
49	MOL002879	Diop	0.39	Scutellariae Radix
50	MOL003920	Methyl icosanoate	0.22	Scutellariae Radix
51	MOL005224	TETRATETRACONTANE	0.25	Scutellariae Radix
52	MOL005368	Methyl tricosanoate	0.33	Scutellariae Radix
53	MOL006370	5-o-caffeoylquinic acid	0.33	Scutellariae Radix
54	MOL007792	Isomartynoside	0.56	Scutellariae Radix
55	MOL008151	METHYL NONADECANOATE	0.19	Scutellariae Radix
56	MOL008206	Moslosooflavone	0.25	Scutellariae Radix
57	MOL008595	Methyl henicosanoate	0.26	Scutellariae Radix
58	MOL009730	Methyl icos-11-enoate	0.23	Scutellariae Radix
59	MOL009734	Methyl lignocerate	0.37	Scutellariae Radix
60	MOL010415	11,13-Eicosadienoic acid, methyl ester	0.23	Scutellariae Radix
61	MOL012240	2',3',5,7-tetrahydroxyflavone	0.24	Scutellariae Radix
62	MOL012245	5,7,4'-trihydroxy-6-methoxyflavanone	0.27	Scutellariae Radix
63	MOL012246	5,7,4'-trihydroxy-8-methoxyflavanone	0.26	Scutellariae Radix
64	MOL012266	Rivularin	0.37	Scutellariae Radix
65	MOL012267	Scutevulin	0.27	Scutellariae Radix
66	MOL013161	METHYL HEXACOSANOATE	0.43	Scutellariae Radix
67	MOL001955	Heriguard	0.33	Coptidis Rhizoma
68	MOL002890	2-Carboxymethyl-3-prenyl-2,3-epoxy-1,4-naphthoquinone	0.26	Coptidis Rhizoma
69	MOL002893	Trihydroxybufosterocholanic acid	0.84	Coptidis Rhizoma
70	MOL002895	DPEC	0.24	Coptidis Rhizoma
71	MOL002898	Groenlandicine	0.72	Coptidis Rhizoma
72	MOL002903	(R)-Canadine	0.77	Coptidis Rhizoma
73	MOL002904	Berlambine	0.82	Coptidis Rhizoma
74	MOL002905	Zosimin	0.36	Coptidis Rhizoma
75	MOL002906	Corchoroside A	0.69	Coptidis Rhizoma
76	MOL002907	Corchoroside A_qt	0.78	Coptidis Rhizoma
77	MOL000778	6-O-E-Feruloylajugol	0.85	Coptidis Rhizoma
78	MOL000779	6-O-E-Feruloylajugol_qt	0.43	Coptidis Rhizoma

(*Continued*)

Table 2 (Continued).

NO.	Mol ID	Component Name	DL	Herb
79	MOL001845	Clemastanin B_qt	0.38	Coptidis Rhizoma
80	MOL008647	Moupinamide	0.26	Coptidis Rhizoma
81	MOL001965	Dauricine (8CI)	0.37	Phellodendri Chinensis Cortex
82	MOL002329	Javanicin	0.78	Phellodendri Chinensis Cortex
83	MOL002635	(±)-lyoniresinol	0.54	Phellodendri Chinensis Cortex
84	MOL002636	Kihadalactone A	0.82	Phellodendri Chinensis Cortex
85	MOL002637	Obacunoic acid	0.79	Phellodendri Chinensis Cortex
86	MOL013352	Obacunone	0.77	Phellodendri Chinensis Cortex
87	MOL002640	Phellavin	0.83	Phellodendri Chinensis Cortex
88	MOL002641	Phellavin_qt	0.44	Phellodendri Chinensis Cortex
89	MOL002642	Phellodendrine	0.58	Phellodendri Chinensis Cortex
90	MOL002643	Delta 7-stigmastenol	0.75	Phellodendri Chinensis Cortex
91	MOL002644	Phellopterin	0.28	Phellodendri Chinensis Cortex
92	MOL002646	Vanilloloside	0.21	Phellodendri Chinensis Cortex
93	MOL002649	Coniferin	0.27	Phellodendri Chinensis Cortex
94	MOL002651	Dehydrotanshinone II A	0.4	Phellodendri Chinensis Cortex
95	MOL002652	Delta7-Dehydrosophoramine	0.25	Phellodendri Chinensis Cortex
96	MOL002654	Amurensin	0.83	Phellodendri Chinensis Cortex
97	MOL002655	Amurensin_qt	0.44	Phellodendri Chinensis Cortex
98	MOL002656	Dihydroniloticin	0.81	Phellodendri Chinensis Cortex
99	MOL002657	Hispidol B	0.81	Phellodendri Chinensis Cortex
100	MOL002658	Kihadalactone B	0.79	Phellodendri Chinensis Cortex
101	MOL002659	Kihadanin A	0.7	Phellodendri Chinensis Cortex
102	MOL002660	Niloticin	0.82	Phellodendri Chinensis Cortex
103	MOL002661	nomilin	0.67	Phellodendri Chinensis Cortex
104	MOL002662	Rutaecarpine	0.6	Phellodendri Chinensis Cortex
105	MOL002663	Skimmianin	0.2	Phellodendri Chinensis Cortex
106	MOL002666	Chelerythrine	0.78	Phellodendri Chinensis Cortex
107	MOL002669	Campesteryl ferulate	0.59	Phellodendri Chinensis Cortex
108	MOL002670	Cavidine	0.81	Phellodendri Chinensis Cortex
109	MOL002671	Candletoxin A	0.69	Phellodendri Chinensis Cortex
110	MOL002672	Hericenone H	0.63	Phellodendri Chinensis Cortex
111	MOL002673	Hispidone	0.83	Phellodendri Chinensis Cortex
112	MOL000347	Syrian	0.32	Phellodendri Chinensis Cortex
113	MOL000741	(2S,3S)-3,5,7-trihydroxy-2- (4-hydroxyphenyl)chroman-4-one	0.24	Phellodendri Chinensis Cortex
114	MOL000762	Palmidin A	0.65	Phellodendri Chinensis Cortex
115	MOL000764	Magnoflorine	0.55	Phellodendri Chinensis Cortex
116	MOL000782	Menisporphine	0.52	Phellodendri Chinensis Cortex
117	MOL000787	Fumarine	0.83	Phellodendri Chinensis Cortex
118	MOL000790	Isocorypalmine	0.59	Phellodendri Chinensis Cortex
119	MOL000508	Friedelin	0.76	Phellodendri Chinensis Cortex
120	MOL000786	STOCK1N-14407	0.64	Phellodendri Chinensis Cortex
121	MOL000794	Menisperine	0.59	Phellodendri Chinensis Cortex
122	MOL001131	Phellamurin_qt	0.39	Phellodendri Chinensis Cortex
123	MOL001455	(S)-Canadine	0.77	Phellodendri Chinensis Cortex
124	MOL001771	Poriferast-5-en-3beta-ol	0.75	Phellodendri Chinensis Cortex
125	MOL003959	Limonin	0.57	Phellodendri Chinensis Cortex
126	MOL004368	Hyperion	0.77	Phellodendri Chinensis Cortex
127	MOL005438	Campesterol	0.71	Phellodendri Chinensis Cortex
128	MOL006276	SMR000232320	0.81	Phellodendri Chinensis Cortex

(*Continued*)

Table 2 (Continued).

NO.	Mol ID	Component Name	DL	Herb
129	MOL006314	Canthin-6-one	0.22	Phellodendri Chinensis Cortex
130	MOL006384	4-[(1R,3aS,4R,6aS)-4-(4-hydroxy-3,5-dimethoxyphenyl)-1,3,3a,4,6,6a-hexahydrofuro[4,3-c]furan-1-yl]-2,6-dimethoxyphenol	0.72	Phellodendri Chinensis Cortex
131	MOL006392	Dihydroniloticin	0.82	Phellodendri Chinensis Cortex
132	MOL006401	Melianone	0.78	Phellodendri Chinensis Cortex
133	MOL006413	Phellochin	0.82	Phellodendri Chinensis Cortex
134	MOL006422	Thalifendine	0.73	Phellodendri Chinensis Cortex
135	MOL006423	Vanilloloside	0.21	Phellodendri Chinensis Cortex
136	MOL013434	Auraptene	0.24	Phellodendri Chinensis Cortex
137	MOL000789	Jatrorrizine	0.59	Coptidis Rhizoma, Phellodendri Chinensis Cortex, Scutellariae Radix
138	MOL001458	Coptisine	0.86	Coptidis Rhizoma, Phellodendri Chinensis Cortex, Scutellariae Radix
139	MOL001454	Berberine	0.78	Coptidis Rhizoma, Phellodendri Chinensis Cortex
140	MOL001457	Columbamine	0.59	Coptidis Rhizoma, Phellodendri Chinensis Cortex
141	MOL002891	Magnoflorine	0.55	Coptidis Rhizoma, Phellodendri Chinensis Cortex
142	MOL002894	Berberrubine	0.73	Coptidis Rhizoma, Phellodendri Chinensis Cortex
143	MOL002901	Phellodendrine	0.58	Coptidis Rhizoma, Phellodendri Chinensis Cortex
144	MOL000622	Magnograndiolide	0.19	Coptidis Rhizoma, Phellodendri Chinensis Cortex
145	MOL000785	Palmatine	0.65	Coptidis Rhizoma, Phellodendri Chinensis Cortex
146	MOL000098	Quercetin	0.28	Coptidis Rhizoma, Phellodendri Chinensis Cortex
147	MOL002668	Worenine	0.87	Coptidis Rhizoma, Phellodendri Chinensis Cortex
148	MOL002897	Epiberberine	0.78	Coptidis Rhizoma, Scutellariae Radix
149	MOL000357	Sitogluside	0.62	Phellodendri Chinensis Cortex, Scutellariae Radix
150	MOL000358	Beta-sitosterol	0.75	Phellodendri Chinensis Cortex, Scutellariae Radix
151	MOL000449	Stigmasterol	0.76	Phellodendri Chinensis Cortex, Scutellariae Radix

target" network diagram (Figure 2). The network consists of 382 nodes and 2116 edges. Of these, Scutellariae Radix (49) is marked with a blue regular octagon, Coptidis Rhizoma (9) is marked with a pink regular octagon, and Phellodendri Chinensis Cortex (29) is marked with a green regular octagon. The chemical composition and attribution of Chinese medicines represented by the letters in the figure are shown in Table 3.

The edges between nodes and nodes indicate the interaction relationship between active components and targets, and larger nodes are significant. From degree analysis, the top 10 compounds were quercetin, apigenin, beta-sitosterol, stigmasterol, magnoflorine, wogonin, columbamine, palmatine, baicalein, and isocorypalmine. Degree was 303, 79, 76, 64, 50, 46, 44, 40, 38, and 37, respectively.

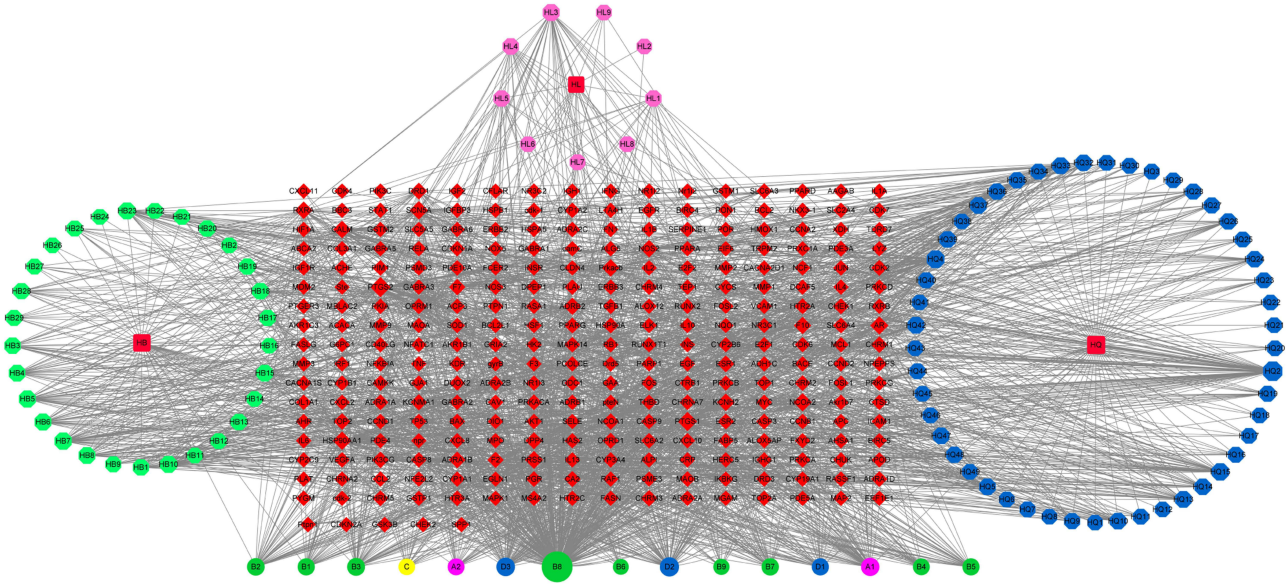

Figure 2 Network diagram of active ingredients and targets of Sanhuang ointment. The size of the node represents the degree value. The typical ingredients of Scutellariae Radix baicalensis, Coptidis Rhizoma, and Phellodendri Chinensis Cortex are marked with purple circles. The common elements between Coptidis Rhizoma and Phellodendri Chinensis Cortex are marked with green circles, Coptidis Rhizoma and Scutellariae Radix baicalensis are marked with a yellow circle, and Phellodendri Chinensis Cortex and Scutellariae Radix baicalensis are marked with a blue circle. The target of the active ingredient (275) are marked with red diamonds.

Potential Targets for Sanhuang Ointment in the Treatment of MRSA Infections of the Skin and Soft Tissue

A total of 329 MRSA infection-related gene targets were identified using Gene cards, OMIM, TTD, Drug bank, and DisGeNET databases. The Venny tool was used to intersect the selected active ingredient targets of Sanhuang ointment with MRSA infection targets to obtain 34 common targets of Sanhuang ointment and MRSA infection.

Table 3 Drug Ingredients Represented by Letters and Assignments

MOL ID	Numbering	Ascription
MOL000007	HQ1	Scutellariae Radix
MOL000008	HQ2	Scutellariae Radix
MOL000073	HQ3	Scutellariae Radix
MOL000173	HQ4	Scutellariae Radix
MOL000228	HQ5	Scutellariae Radix
MOL000359	HQ6	Scutellariae Radix
MOL000396	HQ7	Scutellariae Radix
MOL000458	HQ8	Scutellariae Radix
MOL000525	HQ9	Scutellariae Radix
MOL000552	HQ10	Scutellariae Radix
MOL000870	HQ11	Scutellariae Radix
MOL001490	HQ12	Scutellariae Radix
MOL001689	HQ13	Scutellariae Radix
MOL002560	HQ14	Scutellariae Radix
MOL002714	HQ15	Scutellariae Radix
MOL002737	HQ16	Scutellariae Radix
MOL002819	HQ17	Scutellariae Radix
MOL002879	HQ18	Scutellariae Radix
MOL002909	HQ19	Scutellariae Radix
MOL002910	HQ20	Scutellariae Radix

(*Continued*)

Table 3 (Continued).

MOL ID	Numbering	Ascription
MOL002912	HQ21	Scutellariae Radix
MOL002913	HQ22	Scutellariae Radix
MOL002914	HQ23	Scutellariae Radix
MOL002915	HQ24	Scutellariae Radix
MOL002916	HQ25	Scutellariae Radix
MOL002917	HQ26	Scutellariae Radix
MOL002918	HQ27	Scutellariae Radix
MOL002919	HQ28	Scutellariae Radix
MOL002923	HQ29	Scutellariae Radix
MOL002924	HQ30	Scutellariae Radix
MOL002925	HQ31	Scutellariae Radix
MOL002927	HQ32	Scutellariae Radix
MOL002928	HQ33	Scutellariae Radix
MOL002931	HQ34	Scutellariae Radix
MOL002932	HQ35	Scutellariae Radix
MOL002933	HQ36	Scutellariae Radix
MOL002934	HQ37	Scutellariae Radix
MOL002935	HQ38	Scutellariae Radix
MOL002936	HQ39	Scutellariae Radix
MOL002937	HQ40	Scutellariae Radix
MOL006370	HQ41	Scutellariae Radix
MOL008206	HQ42	Scutellariae Radix
MOL010415	HQ43	Scutellariae Radix
MOL012240	HQ44	Scutellariae Radix
MOL012245	HQ45	Scutellariae Radix
MOL012246	HQ46	Scutellariae Radix
MOL012266	HQ47	Scutellariae Radix
MOL012267	HQ48	Scutellariae Radix
MOL013068	HQ49	Scutellariae Radix
MOL002898	HL1	Coptidis Rhizoma
MOL003959	HL2	Coptidis Rhizoma
MOL002903	HL3	Coptidis Rhizoma
MOL002904	HL4	Coptidis Rhizoma
MOL002905	HL5	Coptidis Rhizoma
MOL002907	HL6	Coptidis Rhizoma
MOL000778	HL7	Coptidis Rhizoma
MOL000779	HL8	Coptidis Rhizoma
MOL001845	HL9	Coptidis Rhizoma
MOL000347	HB1	Phellodendri Chinensis Cortex
MOL000741	HB2	Phellodendri Chinensis Cortex
MOL000764	HB3	Phellodendri Chinensis Cortex
MOL000782	HB4	Phellodendri Chinensis Cortex
MOL000786	HB5	Phellodendri Chinensis Cortex
MOL000787	HB6	Phellodendri Chinensis Cortex
MOL000790	HB7	Phellodendri Chinensis Cortex
MOL000794	HB8	Phellodendri Chinensis Cortex
MOL001131	HB9	Phellodendri Chinensis Cortex
MOL001455	HB10	Phellodendri Chinensis Cortex
MOL001771	HB11	Phellodendri Chinensis Cortex
MOL001965	HB12	Phellodendri Chinensis Cortex

(*Continued*)

Table 3 (Continued).

MOL ID	Numbering	Ascription
MOL002635	HB13	Phellodendri Chinensis Cortex
MOL002641	HB14	Phellodendri Chinensis Cortex
MOL002642	HB15	Phellodendri Chinensis Cortex
MOL002643	HB16	Phellodendri Chinensis Cortex
MOL002644	HB17	Phellodendri Chinensis Cortex
MOL002651	HB18	Phellodendri Chinensis Cortex
MOL002655	HB19	Phellodendri Chinensis Cortex
MOL002662	HB20	Phellodendri Chinensis Cortex
MOL002663	HB21	Phellodendri Chinensis Cortex
MOL002666	HB22	Phellodendri Chinensis Cortex
MOL002670	HB23	Phellodendri Chinensis Cortex
MOL002672	HB24	Phellodendri Chinensis Cortex
MOL004368	HB25	Phellodendri Chinensis Cortex
MOL005438	HB26	Phellodendri Chinensis Cortex
MOL006384	HB27	Phellodendri Chinensis Cortex
MOL006422	HB28	Phellodendri Chinensis Cortex
MOL013434	HB29	Phellodendri Chinensis Cortex
MOL000789	A1	Coptidis Rhizoma, Phellodendri Chinensis Cortex, Scutellariae Radix
MOL001458	A2	Coptidis Rhizoma, Phellodendri Chinensis Cortex, Scutellariae Radix
MOL001454	B1	Coptidis Rhizoma, Phellodendri Chinensis Cortex
MOL001457	B2	Coptidis Rhizoma, Phellodendri Chinensis Cortex
MOL002891	B3	Coptidis Rhizoma, Phellodendri Chinensis Cortex
MOL002894	B4	Coptidis Rhizoma, Phellodendri Chinensis Cortex
MOL002901	B5	Coptidis Rhizoma, Phellodendri Chinensis Cortex
MOL000622	B6	Coptidis Rhizoma, Phellodendri Chinensis Cortex
MOL000785	B7	Coptidis Rhizoma, Phellodendri Chinensis Cortex
MOL000098	B8	Coptidis Rhizoma, Phellodendri Chinensis Cortex
MOL002668	B9	Coptidis Rhizoma, Phellodendri Chinensis Cortex
MOL002897	C	Coptidis Rhizoma, Scutellariae Radix
MOL000357	D1	Phellodendri Chinensis Cortex, Scutellariae Radix
MOL000358	D2	Phellodendri Chinensis Cortex, Scutellariae Radix
MOL000449	D3	Phellodendri Chinensis Cortex, Scutellariae Radix

Construction and Analysis of the Interaction Network

To comprehensively investigate the core pharmacological mechanism of Sanhuang ointment in treating skin and soft tissue MRSA infections, we constructed a protein–protein interaction (PPI) network using overlapping genes. The network has 22 nodes 3 3 edges, and the first three bases of the network diagram are TNF, IL-6, and IL-1β. The size

and color of gene nodes are related to the degree value, and the thickness and color of the connecting lines are related to the correlation between nodes. The larger the node, the darker the color, the more important the node is in the network, and the greater the correlation between the nodes, the thicker the connection line, and the darker the color (Figure 3).

Enrichment Analysis of Sanhuang Ointment for the Therapeutic Targets in Skin and Soft Tissue MRSA Infections

GO functional and KEGG pathway enrichment analysis of the 34 common targets was performed using the DAVID database to further understand the pharmacological mechanisms of Sanhuang ointment against MRSA in skin and soft tissue infections. The threshold was set at $p < 0.05$. We found that biological process functions were mainly related to inflammatory responses, responses to xenogeneic stimuli, and defense responses to bacteria. Cellular components were mainly associated with membrane rafts, membrane microdomains, and plasma membrane rafts. The molecular function was mainly related to cytokine activity, heme binding, and protein homodimer activity (Figure 4). The results of KEGG analysis showed that treatment with Sanhuang ointment for MRSA infection mainly targeted the inflammatory response. The top 10 pathways were the AGE-RAGE signaling pathway in diabetic complications, fluid shear stress and

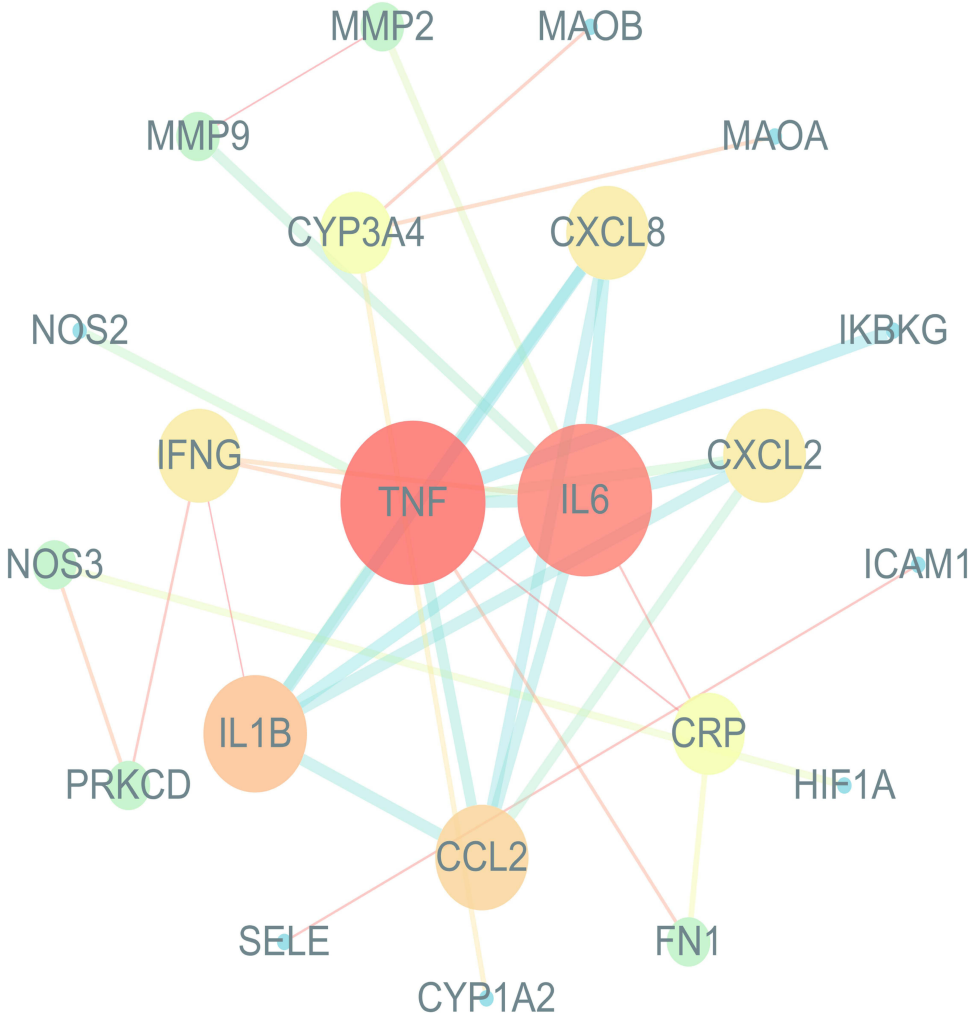

Figure 3 Protein–Protein interaction network. (Matrix metalloproteinase9 (MMP9); 72 kDa type IV collagenase (MMP2); Amine oxidase [flavin-containing] B (MAOB); Amine oxidase [flavin-containing] A (MAOA); Cytochrome P450 3A43 (CYP3A4); Interleukin-8 (CXCL8); Nitric oxide synthase 2 (NOS2); NF-kappa-B essential modulator (IKBKG); Interferon gamma (IFNG); Tumor necrosis factor (TNF); Interleukin-6 (IL6); C-X-C motif chemokine 2 (CXCL2); Nitric oxide synthase 3 (NOS3); Intercellular adhesion molecule 1 (ICAM1); Interleukin-1 beta (IL1B); C-reactive protein (CRP); Protein kinase C delta type (PRKCD); C-C motif chemokine 2 (CCL2); Hypoxia-inducible factor 1-alpha (HIF1A); E-selectin (SELE); Cytochrome P450 1A2 (CYP1A2); Fibronectin (FN1)).

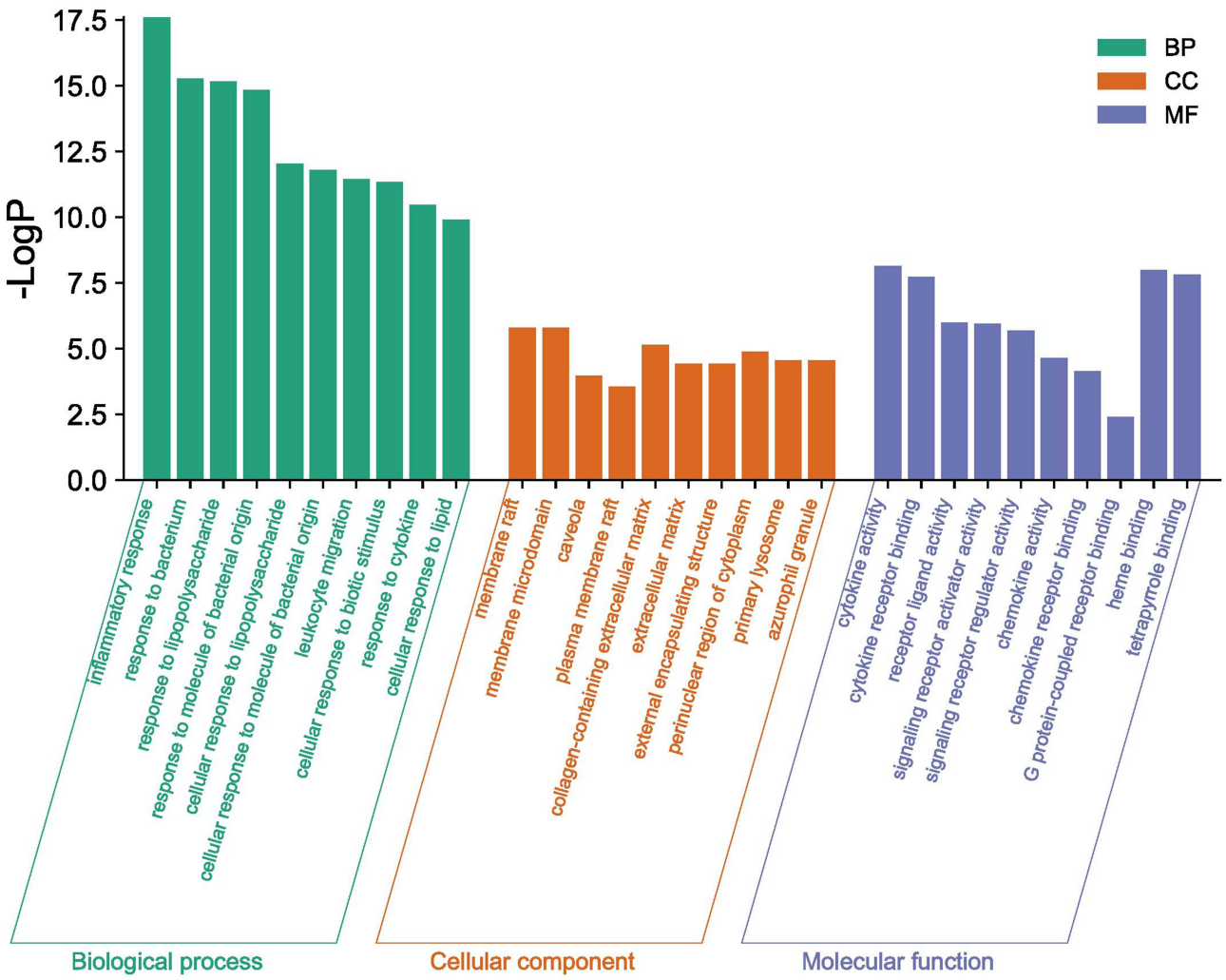

Figure 4 GO enrichment analysis of 34 crosspoint targets. The X-axis represents the top 10 significantly enriched biological processes, cellular components, and molecular functions. The Y-axis represents -log p-values.

atherosclerosis, lipid and atherosclerosis, pathways in cancer, IL-17 signaling pathway, Chagas disease, TNF-α signaling pathway, malaria, and rheumatoid arthritis (Figure 5).

Screening of Bioactive Compounds via UPLC-MS/MS Analysis

Using UPLC-MS/MS analysis, we identified 743 bioactive compounds in Sanhuang ointment (Table 4). Of these, some important bioactive compounds were quercetin, apigenin, beta-sitosterol, stigmasterol, magnoflorine, wogonin, columbamine, palmatine, baicalein, and isocorypalmine.

Pathological Changes in Infected Skin Tissues

The skin tissue structure of rats in the blank group was clear. In the model group, the squamous epithelium of the epidermal layer of the skin tissue was generally thickened. Further, the epidermal structure in the abscess area was destroyed and the level was unclear; the dermis layer became thinner and the staining deepened. The collagen fibers accumulate into sheets and clumps, and a large number of inflammatory cells infiltrated in each layer; the subcutaneous tissue structure is reduced. In the Sanhuang ointment high-dose group, the collagen fiber accumulation in the infected tissue was significantly reduced, the surrounding granulation tissue was filled, and new thin-walled capillaries were observed. In Sanhuang ointment low-dose group, the degree of injury of infected tissue was more serious compared with

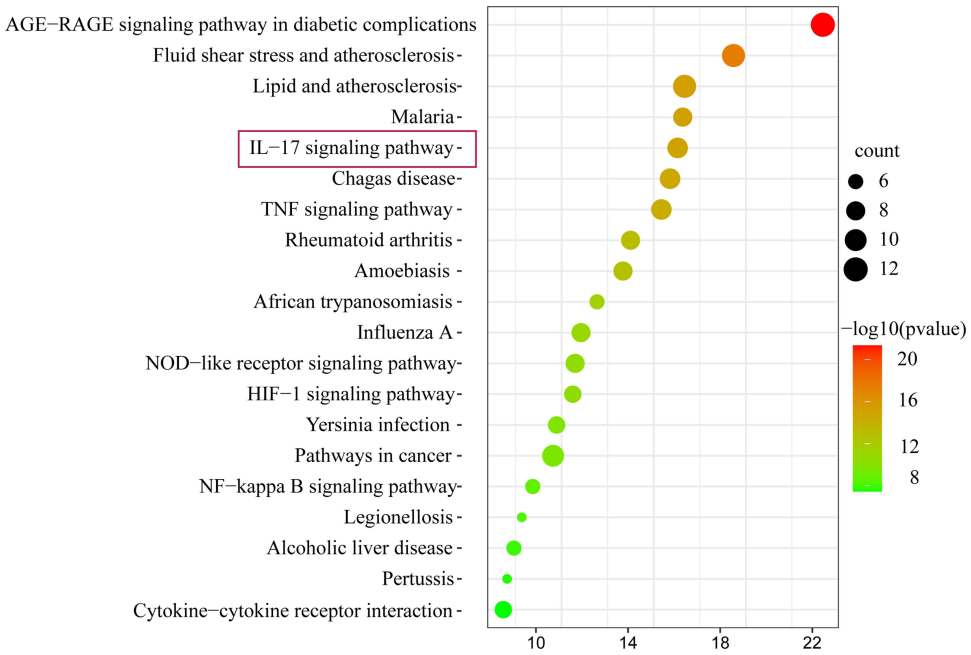

Figure 5 KEGG enrichment analysis of 34 crosspoint targets. The Y-axis represents the top 20 significantly enriched pathways. The X-axis shows the ratio of enriched target genes to background genes. The size of the dots indicates the number of target genes in the pathway, and their color range reflects the different p-values.

that in the high-dose group. Further, collagen fibers accumulated into cords and the necrotic layer was more prominent compared with that in the high-dose group. The granulation tissue filling was less than that seen in Sanhuang ointment high-dose group (Figure 6).

Determination of the Contents of Interleukin IL-1β, IL-4, IL-5, IL-6, IL-17, TNF-α, and IFN-γ in Serum and Skin Tissues of Rats by ELISA

Compared with the blank group, the model group showed significantly increased levels of IL-1β, IL-4, IL-5, IL-6, IL-6, IL-17, TNF-α, and IFN-γ in the serum and skin tissues ($P < 0.01$); compared with the model group, the Sanhuang ointment high- and medium-dose groups showed significantly reduced levels of IL-1β, IL-4, IL-5, IL-6, IL-6, IL-17, TNF-α, and IFN-γ in the serum and skin tissues ($P < 0.05$, $P < 0.01$). The results are shown in Figure 7.

Expression Levels of IL-1β, IL-4, IL-5, IL-6, IL-17, TNF-α, TRAF6, TAK1, TAB1, IKK β, NF-κB p65 mRNA in Rat Skin Tissues

Compared with the blank group, the model groups showed significantly increased levels of IL-1β, IL-4, IL-5, IL-6, IL-17, TNF-α, TRAF6, TAK1, TAB1, IKKβ, and NF-κB p65 mRNA in the skin tissue of rats ($P < 0.01$); compared with the model group, the Sanhuang ointment high- and medium-dose groups showed significantly decreased levels of IL-1β, IL-4, IL-5, IL-6, IL-17, TNF-α, TRAF6, TAK1, TAB1, IKKβ, and NF-κB p65 mRNA in the skin tissue of rats ($P < 0.05$, $P < 0.01$). Results are shown in Figure 8.

TRAF6, TAB1, TAK1, IKK β, and NF-κB p65 Protein in Infected Rat Skin Tissues

Compared with the blank group, the model group showed significantly increased expression levels of TNF receptor-associated factor 6, transforming growth factor kinase 1, transforming growth factor kinase 1 binding protein 1, kappa B inhibitor kinase β, and NF-κB p65 protein in the skin tissue of rats ($P < 0.01$); further, compared with the model group, the Sanhuang ointment high- and medium-dose groups showed significantly decreased expression levels of NF-κB p65 protein in the skin tissue of rats ($P < 0.05$, $P < 0.01$). The results are shown in Figure 9.

Table 4 The Chemical Constituents and Related Information of Sanhuang Ointment

MOL ID	Q1 (Da)	Q3 (Da)	Molecular Weight (Da)	Formula	Ionization Model	Compounds	Class I	Class II	CAS	Level	A	cpd_ID
MOL004194	356.1862	192.1043	355.1784	C21H25NO4	[M+H]+	Corybulbine	Alkaloids	Isoquinoline alkaloids	518-77-4	1	651829460.7	-
MOL002898	322.1074	307.0944	322.1074	C19H16NO4+	[M]+	Groenlandicine	Alkaloids	Isoquinoline alkaloids	38691-95-1	1	503515511.1	-
MOL013066	431.0993	255.07	430.09	C21H18O10	[M+H]+	Chrysin-7-O-Glucuronide	Flavonoids	Flavones	35775-49-6	1	502005790.1	-
MOL000764	342.17	297.1129	342.17	C20H24NO4+	[M]+	Magnoflorine	Alkaloids	Aporphine alkaloids	2141-09-5	1	475325298.3	C09581
MOL002714	271.0601	123.0077	270.0528	C15H10O5	[M+H]+	Baicalein	Flavonoids	Flavones	491-67-8	1	378874658.9	C10023
MOL000794	356.1856	279.1033	356.1856	C21H26NO4+	[M]+	Menisperine	Alkaloids	Aporphine alkaloids	25342-82-9	1	346121500.6	-
MOL000785	352.1543	337.097	352.1543	C21H22NO4+	[M]+	Palmatine	Alkaloids	Isoquinoline alkaloids	3486-67-7	1	317732457	C05315
MOL003959	471.2019	425.1952	470.1941	C26H30O8	[M+H]+	Limonin	Terpenoids	Triterpene	1180-71-8	1	281789235.4	C03514
MOL000173	285.0758	270.0654	284.0685	C16H12O5	[M+H]+	Wogonin (5,7-Dihydroxy-8-Methoxyflavone)	Flavonoids	Flavones	632-85-9	1	225808187.2	C10197
MOL001455	340.1543	325.1203	339.1471	C20H21NO4	[M+H]+	(S)-Canadine	Alkaloids	Isoquinoline alkaloids	5096-57-1	1	221948182.7	C03329
MOL013352	455.2064	409.2005	454.1992	C26H30O7	[M+H]+	Obacunone	Terpenoids	Triterpene	751-03-1	1	128784863.4	C08775
MOL009754	433.1129	271.0599	432.1056	C21H20O10	[M+H]+	Oroxin A	Flavonoids	Flavones	57396-78-8	1	128411322.9	-
MOL002776	447.0922	271.062	446.0849	C21H18O11	[M+H]+	Baicalin	Flavonoids	Flavones	21967-41-9	1	127020412.2	C10025
MOL002901	342.1719	192.1022	342.17	C20H24NO4+	[M]+	Phellodendrine	Alkaloids	Isoquinoline alkaloids	6873-13-8	1	118417114.1	C17046
MOL000394	104.107	60.0808	104.107	C5H14NO+	[M]+	Choline	Alkaloids	Alkaloids	62-49-7	1	115827008.4	C00114
MOL000676	279.1588	149.0249	278.1518	C16H22O4	[M+H]+	Dibutyl phthalate	Phenolic acids	Phenolic acids	84-74-2	1	108880435.2	C14214
MOL003871	353.0878	191.0553	354.0951	C16H18O9	[M-H]-	Chlorogenic acid (3-O-Caffeoylquinic acid)*	Phenolic acids	Phenolic acids	327-97-9	1	76357495.49	C00852
MOL004197	342.17	297.1125	341.1627	C20H23NO4	[M+H]+	Corydine*	Alkaloids	Aporphine alkaloids	476-69-7	1	65108121.03	-
MOL003065	353.0878	191.0561	354.0951	C16H18O9	[M-H]-	Cryptochlorogenic acid (4-O-Caffeoylquinic acid)*	Phenolic acids	Phenolic acids	905-99-7	1	58671695.66	-
MOL008250	149.0233	65.0406	148.016	C8H4O3	[M+H]+	Phthalic anhydride	Phenolic acids	Phenolic acids	85-44-9	1	44686358.59	-
MOL002084	493.1341	331.0812	492.1268	C23H24O12	[M+H]+	Tricin-7-O-Glucoside	Flavonoids	Flavones	32769-01-0	1	40919729.08	-
MOL000239	313.0718	283.0248	314.079	C17H14O6	[M-H]-	5,4'-Dihydroxy-3,7-dimethoxyflavone(Kumatakenin)	Flavonoids	Flavonols	3301-49-3	1	40338583.31	-
MOL000360	193.0506	134.0373	194.0579	C10H10O4	[M-H]-	Ferulic acid*	Phenolic acids	Phenolic acids	537-98-4	1	37026226.65	C01494
MOL005928	193.0506	134.0374	194.0579	C10H10O4	[M-H]-	Isoferulic Acid*	Phenolic acids	Phenolic acids	25522-33-2	1	33112337.9	C10470

(*Continued*)

https://doi.org/10.2147/IDR.S424746

Table 4 (Continued).

MOL ID	Q1 (Da)	Q3 (Da)	Molecular Weight (Da)	Formula	Ionization Model	Compounds	Class I	Class II	CAS	Level	A	cpd_ID
MOL006370	353.0878	191.0561	354.0951	C16H18O9	[M-H]-	Neochlorogenic acid (5-O-Caffeoylquinic acid)*	Phenolic acids	Phenolic acids	906-33-2	I	30003807.67	C17147
MOL010864	345.0969	284.0713	344.0896	C18H16O7	[M+H]+	5,7-Dihydroxy-3',4',5'-trimethoxyflavone	Flavonoids	Flavones	18103-42-9	I	23296631.69	C19807
MOL001842	357.1344	151.0384	358.1416	C20H22O6	[M-H]-	Pinoresinol*	Lignans and Coumarins	Lignans	487-36-5	I	21992285.4	C05366
MOL011338	357.1344	151.0442	358.1416	C20H22O6	[M-H]-	Epipinoresinol*	Lignans and Coumarins	Lignans	24404-50-0	I	19685265.35	-
MOL002932	315.0863	271.0601	314.079	C17H14O6	[M+H]+	5,2'-Dihydroxy-7,8-dimethoxyflavone	Flavonoids	Flavones	41060-16-6	I	12160062.35	-
MOL009149	326.1398	311.1167	325.1314	C19H19NO4	[M+H]+	Cheilanthifoline	Alkaloids	Isoquinoline alkaloids	483-44-3	I	11370081.29	C05174
MOL000006	287.055	153.0188	286.0477	C15H10O6	[M+H]+	Luteolin (5,7,3',4'-Tetrahydroxyflavone)	Flavonoids	Flavones	491-70-3	I	9189132.702	C01514
MOL007998	461.0743	285.0409	462.0798	C21H18O12	[M-H]-	Kaempferol-3-O-glucuronide	Flavonoids	Flavonols	22688-78-4	I	8484332.685	-
MOL007206	314.1751	283.133	313.1678	C19H23NO3	[M+H]+	Armepavine	Alkaloids	Isoquinoline alkaloids	524-20-9	I	4885679.957	C09342
MOL002653	200.0663	185.05	199.0633	C12H9NO2	[M+H]+	Dictamine	Alkaloids	Quinoline alkaloids	484-29-7	I	4736662.639	C10660
MOL002560	255.0643	153.0175	254.0579	C15H10O4	[M+H]+	Chrysin	Flavonoids	Flavones	480-40-0	I	3895697.273	C10028
MOL009774	329.0667	314.0432	330.074	C17H14O7	[M-H]-	3,7-Di-O-methylquercetin	Flavonoids	Flavonols	2068/2/2	I	3660066.152	C01265
MOL001773	118.0651	91.0542	117.0578	C8H7N	[M+H]+	Indole	Alkaloids	Plumerane	120-72-9	I	2355538.033	C00463
MOL006263	485.1806	381.1544	484.1733	C26H28O9	[M+H]+	Evodol	Terpenoids	Triterpene	22318-10-1	I	2171327.964	-
MOL002331	242.1176	227.0941	241.1103	C15H15NO2	[M+H]+	N-Methylflindersine	Alkaloids	Isoquinoline alkaloids	50333-13-6	I	2104487.876	C10731
MOL001522	286.1443	107.0533	285.1365	C17H19NO3	[M+H]+	Coclaurine	Alkaloids	Isoquinoline alkaloids	486-39-5	I	1840309.887	C06161
MOL009763	579.2084	417.1564	580.2156	C28H36O13	[M-H]-	Syringaresinol-4'-O-glucoside	Lignans and Coumarins	Lignans	7374-79-0	I	1643811.129	C10890
MOL005559	471.348	471.348	472.3553	C30H48O4	[M-H]-	2,3-Dihydroxyurs-12-en-29-oic acid (Maslinic acid)	Terpenoids	Triterpene	4373-41-5	I	1263913.301	C16939
MOL012969	471.348	471.3502	472.3553	C30H48O4	[M-H]-	2,3-Dihydroxyolean-12-en-28-oic acid (2-Hydroxyoleanolic acid)	Terpenoids	Triterpene	26707-60-8	I	1251632.571	-
MOL005080	169.0495	65.0022	168.0423	C8H8O4	[M+H]+	2,6-Dimethoxy-1,4-benzoquinone	Quinones	Quinones	530-55-2	I	1186778.655	C10331
MOL002844	255.0663	151.0035	256.0736	C15H12O4	[M-H]-	Pinocembrin (Dihydrochrysin)	Flavonoids	Flavanones	480-39-7	I	1167079.028	C09827
MOL009333	330.17	299.1279	329.1627	C19H23NO4	[M+H]+	Reticuline	Alkaloids	Isoquinoline alkaloids	485-19-8	I	679499.664	C02105

MOL003940	284.2951	102.0909	283.2875	C18H37NO	[M+H]+	Stearamide	Alkaloids	Alkaloids	124-26-5	1	453498.416	C13846
MOL007413	565.1552	529.1341	564.1479	C26H28O14	[M+H]+	Schaftoside	Flavonoids	Flavones	51938-32-0	1	134811.778	C10181
MOL009048	211.0766	169.0654	212.08373	C14H12O2	[M-H]-	Pinosylvin	Others	Stilbene	22139-77-1	1	118094.197	C01745
MOL001895	205.1584	189.1288	206.1671	C14H22O	[M-H]-	2,6-Di-tert-butylphenol*	Phenolic acids	Phenolic acids	128-39-2	1	83204.26	-
MOL002092	205.1598	189.1267	206.1671	C14H22O	[M-H]-	2,4-Di-Tert-Butylphenol*	Phenolic acids	Phenolic acids	96-76-4	1	81433.105	-
MOL000159	625.2109	163.0392	624.2054	C29H36O15	[M+H]+	Isoacteoside*	Phenolic acids	Phenolic acids	61303-13-7	1	69821.658	-
MOL003333	625.211	163.0389	624.2054	C29H36O15	[M+H]+	Acteoside; Verbascoside*	Phenolic acids	Phenolic acids	61276-17-3	1	56511.321	C10501

Notes: MOL ID: Substance ID; Q1: The molecular weight of the parent ion after adding ions by the electrospray ion source; Q3 (Da): Characteristic fragment ion; Molecular weight (Da): Relative molecular mass; Formula: Substance molecular formula; Ionization model: ionization mode (M+H is positively charged, M-H is negatively charged); Compounds: the English name of the substance; the substance: the Chinese name of the substance; Class I: the English first-class category of the substance; the first-class classification of the substance: the Chinese first-class category of the substance; Class II: the secondary category of the substance in English; the secondary classification of the substance: the secondary category of the substance in Chinese; CAS: the CAS number of the substance; Level: the identification level of the substance (1: the secondary mass spectrometry of the sample substance (all fragmented product ions of the substance), RT and The database substance matching score is above 0.7); cpd_ID: substance KEGG database number; kegg_map: KEGG database pathway number; other columns: sample relative content.

https://doi.org/10.2147/IDR.S424746

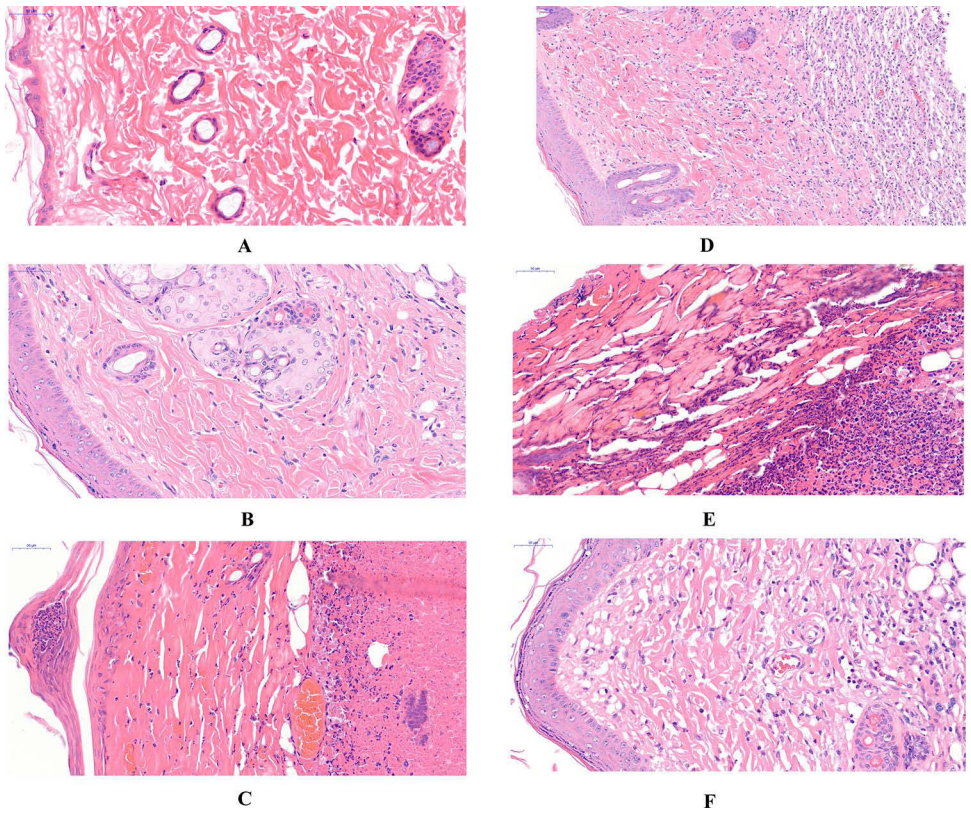

Figure 6 Histomorphology of rat skin in each group (HE staining, 40×).
Notes: (**A**) Blank group; (**B**) Model group; (**C**) Mupirocin Ointment group; (**D**) Sanhuang Ointment high-dose group; (**E**) Sanhuang Ointment medium-dose group; (**F**) Sanhuang Ointment low-dose group.

Discussion

According to the characteristics of clinical symptoms of local soft tissue infection on the body surface, which are often accompanied by "redness, swelling, heat, and pain", it belongs to the category of yang syndrome of "swelling ulcer" in TCM and is mostly treated from the pathogenesis of "heat toxin", with significant effect.

In this study, 275 potential targets of Sanhuang ointment were screened using a network pharmacology approach. In all, 34 common targets were identified on intersecting 329 MRSA infection targets. Enrichment analysis identified 488 biological processes, 32 molecular functions, 20 cellular components, and 76 signaling pathways. We found that the key compounds in the 254 active Sanhuang ointment immune system's response against MRSA infection were as follows: quercetin, apigenin, beta-sitosterol, stigmasterol, magnoflorine, wogonin, columbamine, palmatine, baicalein, and isocorypalmine. By regulating NOS2, IL6, TNF-α, NOS3, CXCL8, IL1B, CCL2, IFNG, IKBKG, ICAM1, and other related target proteins against MRSA infection. These abovementioned components are also involved in regulating key biological pathways, such as inflammation and bacterial infection, and may treat MRSA infection via the IL-17/NF-κB signaling pathway.

IL-17 is an effector cytokine of the innate and adaptive immune systems involved in antimicrobial host defense and tissue integrity maintenance.[29] Signaling through the IL-17RA/IL-17RC heterodimeric receptor complex triggers homotypic interactions of IL-17RA and IL-17RC chains with the TRAF3IP2 linker. This leads to downstream TRAF6-mediated activation of NF-κB and MAP kinase pathways, ultimately resulting in transcriptional activation of cytokines, chemokines, antimicrobial peptides, and interferon matrix metalloproteinases, accompanied by a potentially strong inflammatory response.[29–34] Studies have confirmed that IL-17 expression levels are increased in infected tissues and sera of rats with skin and soft tissue MRSA infections, inducing an inflammatory response and thus the release of other inflammatory factors (ie, IL-1β, IL-4, IL-5, IL-6, TNF-α, and IFN-γ) in rat skin and soft tissue, thereby leading to imbalanced host inflammatory response.[35] NF-κB has pleiotropic regulatory functions and can bind to multiple promoters and participate in the regulation of multiple inflammatory genes.[36] When inflammatory changes occur in the skin and soft tissue, serum IL-17 levels rise,

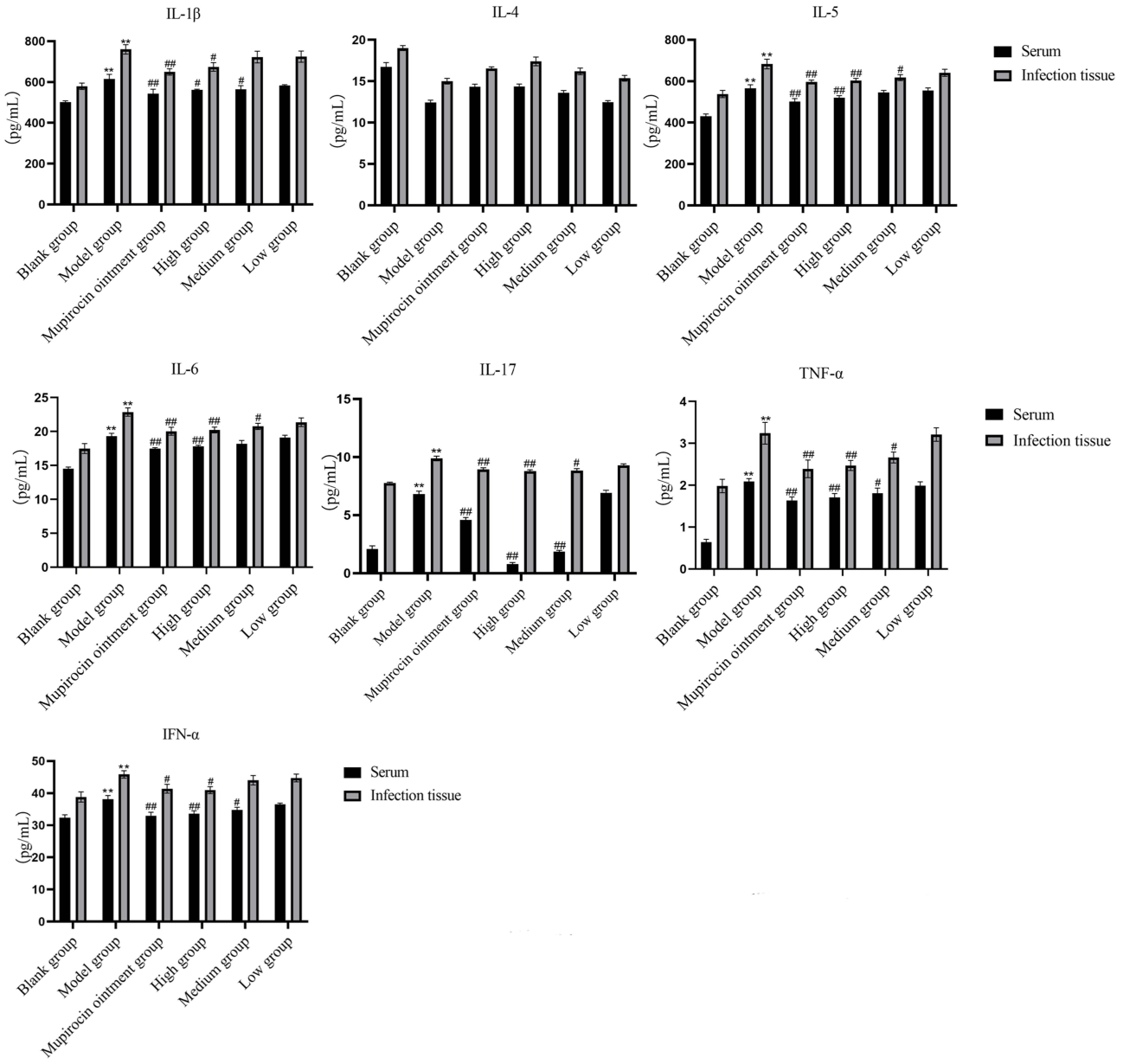

Figure 7 Comparison of IL-1β, IL-4, IL-5, IL-6, IL-17, TNF-α, and IFN-γ contents in the serum and skin tissues of rats in each group (x±s).
Notes: Compared with the blank group, **P<0.01; compared with the model group, #P<0.05, ##P<0.01.

inducing NF-κB activity and promoting inflammation in the skin and soft tissue. Activated NF-κB can in turn reverse promote inflammatory factor expression and lead to further skin and soft tissue injury.[37] TAB1 is an adaptor protein related to the N-terminal kinase domain of transforming growth factor β-activated kinase 1 (TAK1) and is an essential binding protein for sustained TAK1 activation.[38] TAK1 is a key molecule in the IL-17/NF-κB signaling pathway that phosphorylates IκB kinase (IKK) upon binding with TAB1, ultimately leading to the nuclear translocation of the transcription factor NF-κB and promoting downstream inflammatory factor production.[39] Mammalian NF-κB is formed by members of the Rel family of five related proteins that bind to form dimers, including p50 and p65, which contain major NF-κB transcriptional activity. NF-κB is responsible for the expression of a large number of pro-inflammatory mediators and promotes innate immune cell leukocyte recruitment.[37] Accordingly, when the body is infected by microorganisms, an inflammatory response is initiated, inducing the gene expression of a large number of pro-inflammatory cytokines and chemokines through NF-κB activation.[40] The pro-inflammatory cytokines including TNF-α and IL-1β can also directly activate the NF-κB pathway. This positive feedback effect contributes to the amplification of the inflammatory response, which persists at the site of infection and helps

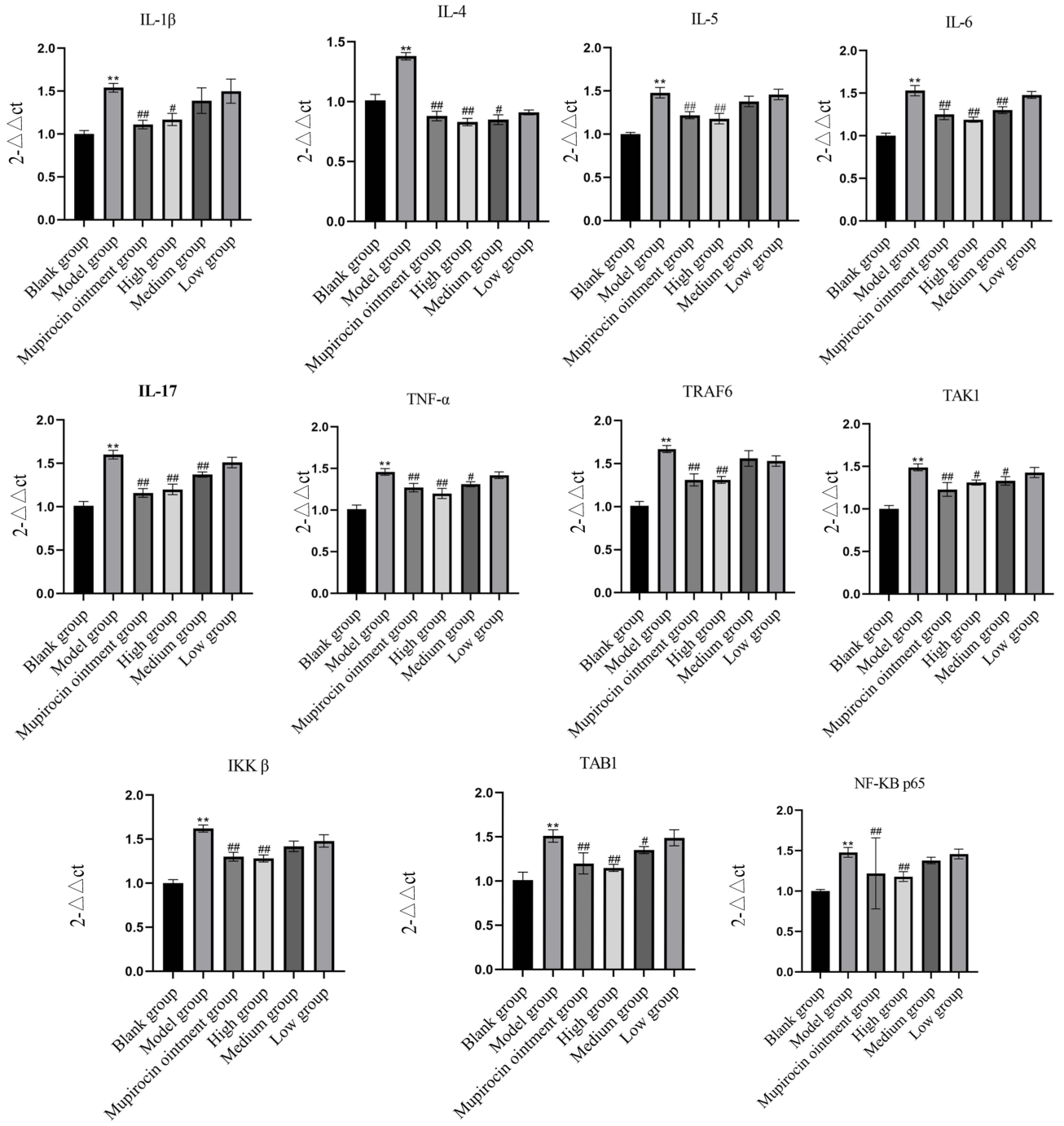

Figure 8 Comparison of IL-1β, IL-4, IL-5, IL-6, IL-17, TNF-α, IFN-γ, TRAF6, TAK1, TAB1, IKKβ, and NF-κB p65 mRNA expression levels in the skin tissue of rats in each group (x±s).

Notes: Compared with the blank group, **P<0.01; compared with the model group, #P<0.05, ##P<0.01.

clear invading pathogens. In contrast, the recruited leukocytes (neutrophils) are quite important for regulating the inflammatory response. Given that neutrophils function in an unfavorable microenvironment, NF-κB regulates the survival of these neutrophils. Further, NF-κB regulates the transcription of many genes, and post-transcriptionally expressed proteins are widely involved in cell adhesion, differentiation, proliferation, angiogenesis, and apoptosis in addition to immune responses and inflammatory responses.[41]

In this study, a rat model of MRSA infection in the skin and soft tissue was designed to observe the effect of the external application of Sanhuang ointment on infected soft tissues. Furthermore, the anti-inflammatory mechanism of

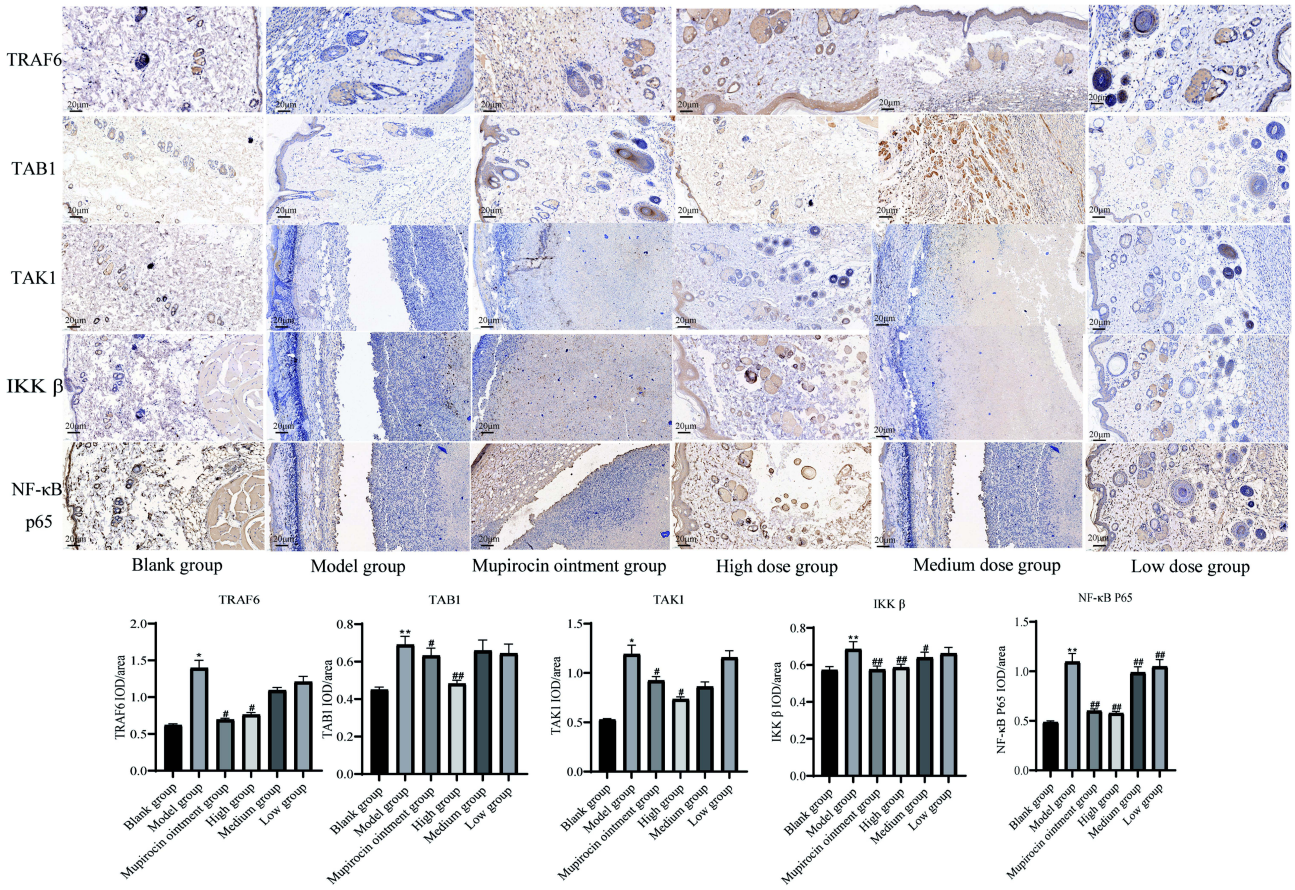

Figure 9 Comparison of TRAF6, TAK1, TAB1, IKKβ, and NF-κB p65 protein expressions in the skin tissues of rats in each group (x±s).
Notes: Compared with the blank group, *P<0.05, **P<0.01; compared with the model group, #P<0.05, ##P<0.01.

Sanhuang ointment was explored based on the pathological changes and the expressions of key molecules of signaling pathways in the serum and infected tissues. The results showed that compared with the blank group, the model group showed significantly increased levels of IL-1β, IL-4, IL-5, IL-6, TNF-α, IFN-γ, and IL-17 downstream inflammatory factors of IL-17/NF-κB signaling pathway in the serum and skin tissues of rats. Protein and mRNA expressions of TRAF6, TAK1, TAB1, IKK, and NF-κB p65 were significantly increased in the model group, suggesting that the skin tissues were significantly infected and an inflammatory response was aggravated. Compared with the model group, the Sanhuang ointment groups showed significantly improved general conditions with improvement in pathological changes in rats. The expression levels of the abovementioned factors were reduced to varying degrees, indicating that Sanhuang ointment external application can reduce MRSA-induced skin and soft tissue inflammation in rats; thus, Sanhuang ointment may play an anti-inflammatory role by inhibiting the expression of key factors of IL-17/NF-κB signaling pathway, thereby reducing the release of downstream pro-inflammatory factors. In this study, the targets of Sanhuang ointment and the involved signal transduction pathways were screened by network pharmacology and verified by animal experiments to reveal the mechanism of action of Sanhuang ointment in the treatment of MRSA infections in the skin and soft tissues, providing a scientific basis and further ideas for future research. The main chemical components of Sanhuang ointment were further verified by LC-MS/MS. The molecular mechanism of its network pharmacology-based anti-skin and soft tissue infection against MRSA was initially elucidated, and further experimental verification is needed.

Conclusion

Sanhuang ointment may inhibit the inflammatory response induced by MRSA in the skin and soft tissue infections by targeting the IL-17/NF-κB signaling pathway. We study the active components and mechanism of action of Sanhuang ointment on MRSA infection through network pharmacology.

Abbreviations

MRSA, Methicillin-resistant Staphylococcus aureus; SSTI, Skin and soft tissue infections; NF-κB, Nuclear factor kappa-B; MAPK, Mitogen-activated protein kinase; NO, Nitrogen monoxide; iNOS, inducible nitric oxide synthase; TLR2, Toll Like Receptor 2; IL-1β, Interleukin 1 beta; IL-4, Interleukin 4; IL-5, Interleukin 5; IL-6, Interleukin 6; IL-17, Interleukin 17; TNF-α, Tumor necrosis factor-alpha; IFN-γ, Interferon-gamma; TRAF6, TNF receptor associated factor 6; TAK1, Transforming growth factor kinase 1; TAB1, Transforming growth factor β-activated kinase 1 binding protein 1; IKKβ, Inhibitor of nuclear factor kappa-B kinase subunit beta.

Data Sharing Statement

All data generated or analyzed during this study are included in this article.

Author Contributions

All authors made a significant contribution to the work reported, whether that is in the conception, study design, execution, acquisition of data, analysis and interpretation, or in all these areas; took part in drafting, revising, or critically reviewing the article; gave final approval of the version to be published; have agreed on the journal to which the article has been submitted; and agree to be accountable for all aspects of the work.

Funding

This research was supported by the National Natural Science Foundation of China (81860850), the Gansu Provincial Department of Education Project (2021CXZX-734 and 2021CXZX-736), and the Gansu Provincial Higher Education Innovation Project (2023S-76).

Disclosure

Haibang Pan and Tianming Wang are co-first authors for this study. The authors declare that they have no known competing financial interests or personal relationships that could have appeared to influence the work reported in this paper.

References

1. Moffarah AS, Al Mohajer M, Hurwitz BL, Armstrong DG. Skin and soft tissue infections. *Microbiol Spectr*. 2016;4(4). doi:10.1128/microbiolspec.DMIH2-0014-2015
2. Lakhundi S, Zhang KY. Methicillin-resistant Staphylococcus aureus: molecular characterization, evolution, and epidemiology. Review. *Clin Microbiol Rev*. 2018;31(4):103. e00020–18. doi:10.1128/cmr.00020-18
3. Turner NA, Sharma-Kuinkel BK, Maskarinec SA, et al. Methicillin-resistant Staphylococcus aureus: an overview of basic and clinical research. Review. *Nat Rev Microbiol*. 2019;17(4):203–218. doi:10.1038/s41579-018-0147-4
4. Bateman A, Martin M-J, Orchard S. UniProt: the universal protein knowledgebase in 2021. *Nucleic Acids Res*. 2021;49(D1):D480–D489. doi:10.1093/nar/gkaa1100
5. Baek JY, Chung DR, Ko KS, et al. Genetic alterations responsible for reduced susceptibility to vancomycin in community-associated MRSA strains of ST72. *J Antimicrob Chemother*. 2017;72(9):2454–2460. doi:10.1093/jac/dkx175
6. Werth BJ, Jain R, Hahn A, et al. Emergence of dalbavancin non-susceptible, vancomycin-intermediate Staphylococcus aureus (VISA) after treatment of MRSA central line-associated bloodstream infection with a dalbavancin- and vancomycin-containing regimen. *Clin Microbiol Infect*. 2018;24(4):429.e1–429.e5. doi:10.1016/j.cmi.2017.07.028
7. Haibang P, Bo W, Xinping W, Guotai W, Hua Y. 2538 cases of common surgical diseases treated by external application of Sanhuang ointment. *J External TreatTrad Chin Med*. 2015;24(02):30–31.
8. Haibang P, Guotai W, Bo Y. Experimental study on anti-inflammatory and analgesic effects of different blends of Sanhuang Tablet. *China Trad Chin Med Technol*. 2015;22(05):502–503.
9. Haibang P, Guotai W, Jianfeng Y, Bo W, Xiaopeng D. Clinical observation of sanhuang ointment in treating local soft tissue infection. *Chin J Exp Formulas*. 2017;23(20):174–179. doi:10.13422/j.cnki.syfjx.2017200174
10. Hao Y, Huo J, Wang T, Sun G, Wang W. Chemical profiling of Coptis rootlet and screening of its bioactive compounds in inhibiting Staphylococcus aureus by UPLC-Q-TOF/MS. *J Pharm Biomed Anal*. 2020;180:113089. doi:10.1016/j.jpba.2019.113089
11. Hwang SJ, Lee HJ. Phenyl-beta-d-glucopyranoside exhibits anti-inflammatory activity in lipopolysaccharide-activated RAW 264.7 cells. Article. *Inflammation*. 2015;38(3):1071–1079. doi:10.1007/s10753-014-0072-2
12. Guven-Maiorov E, Keskin O, Gursoy A, Nussinov R. A structural view of negative regulation of the toll-like receptor-mediated inflammatory pathway. *Biophys J*. 2015;109(6):1214–1226. doi:10.1016/j.bpj.2015.06.048
13. Choi YY, Kim MH, Han JM, et al. The anti-inflammatory potential of Cortex Phellodendron in vivo and in vitro: down-regulation of NO and iNOS through suppression of NF-κB and MAPK activation. *Int Immunopharmacol*. 2014;19(2):214–220. doi:10.1016/j.intimp.2014.01.020

14. Hu ZW, Lin JH, Chen JT, et al. Overview of viral pneumonia associated with influenza virus, respiratory syncytial virus, and coronavirus, and therapeutics based on natural products of medicinal plants. Review. *Front Pharmacol*. 2021;12(21):630834. doi:10.3389/fphar.2021.630834
15. Dinda B, Dinda S, DasSharma S, Banik R, Chakraborty A, Dinda M. Therapeutic potentials of baicalin and its aglycone, baicalein against inflammatory disorders. *Eur J Med Chem*. 2017;131:68–80. doi:10.1016/j.ejmech.2017.03.004
16. Wang H-Z, Yu C-H, Gao J, Zhao G-R. HPLC分析比较炮制和提取方法对黄芩活性成分的影响 [Effects of processing and extracting methods on active components in Radix Scutellariae by HPLC analysis]. *Zhongguo Zhong Yao Za Zhi*. 2007;32(16):1637–1640. Chinese.
17. Liao H, Ye J, Gao L, Liu Y. The main bioactive compounds of Scutellaria baicalensis Georgi. for alleviation of inflammatory cytokines: a comprehensive review. *Biomed Pharmacother*. 2021;133:110917. doi:10.1016/j.biopha.2020.110917
18. Haibang P, Tianming W, Yan C, et al. Effects of sanhuang ointment on subcutaneous soft tissue inflammation and TLR2/ NF-κB signaling pathway in MRSA infection model rats. *Chin J Inform Trad Chin Med*. 2022;29(08):54–59. doi:10.19879/j.cnki.1005-5304.202112157
19. Li S, Zhang ZQ, Wu LJ, Zhang XG, Li YD, Wang YY. Understanding ZHENG in traditional Chinese medicine in the context of neuro-endocrine-immune network. *IET Syst Biol*. 2007;1(1):51–60. doi:10.1049/iet-syb:20060032
20. Li S, Zhang B. Traditional Chinese medicine network pharmacology: theory, methodology and application. *Chin J Nat Med*. 2013;11(2):110–120. doi:10.1016/S1875-5364(13)60037-0
21. Wang SL, Tang C, Zhao H, et al. Network pharmacological analysis and experimental validation of the mechanisms of action of Si-Ni-San against liver fibrosis. Article. *Front Pharmacol*. 2021;12(19):656115. doi:10.3389/fphar.2021.656115
22. Hopkins AL. Network pharmacology: the next paradigm in drug discovery. *Nat Chem Biol*. 2008;4(11):682–690. doi:10.1038/nchembio.118
23. Ru J, Li P, Wang J, et al. TCMSP: a database of systems pharmacology for drug discovery from herbal medicines. *J Cheminform*. 2014;6(1):13. doi:10.1186/1758-2946-6-13
24. Pichler K, Warner K, Magrane M. SPIN: submitting sequences determined at protein level to UniProt. *Curr Protoc Bioinformatics*. 2018;62(1):e52. doi:10.1002/cpbi.52
25. Amberger JS, Bocchini CA, Schiettecatte F, Scott AF, Hamosh A. OMIM.org: Online Mendelian Inheritance in Man (OMIM®), an online catalog of human genes and genetic disorders. *Nucleic Acids Res*. 2015;43(Database issue):D789–D798. doi:10.1093/nar/gku1205
26. Szklarczyk D, Gable AL, Lyon D, et al. STRING v11: protein-protein association networks with increased coverage, supporting functional discovery in genome-wide experimental datasets. *Nucleic Acids Res*. 2019;47(D1):D607–D613. doi:10.1093/nar/gky1131
27. Malachowa N, Kobayashi SD, Lovaglio J, DeLeo FR. Mouse model of Staphylococcus aureus skin infection. *Methods Mol Biol*. 2019;1960:139–147. doi:10.1007/978-1-4939-9167-9_12
28. Wang Z, Gao C, Zhang L, Sui R. Retraction notice to "Hesperidin methylchalcone (HMC) hinders amyloid-β induced Alzheimer's disease by attenuating cholinesterase activity, macromolecular damages, oxidative stress and apoptosis via regulating NF-κB and Nrf2/HO-1 pathways" [Int. J. Biol. Macromol. 233 (2023) 123169]. *Int J Biol Macromol*. 2023;249:125762. doi:10.1016/j.ijbiomac.2023.125762
29. Boisson B, Wang C, Pedergnana V, et al. An ACT1 mutation selectively abolishes interleukin-17 responses in humans with chronic mucocutaneous candidiasis. *Immunity*. 2013;39(4):676–686. doi:10.1016/j.immuni.2013.09.002
30. Liu C, Qian W, Qian Y, et al. Act1, a U-box E3 ubiquitin ligase for IL-17 signaling. *Sci Signal*. 2009;2(92):ra63. doi:10.1126/scisignal.2000382
31. Puel A, Cypowyj S, Bustamante J, et al. Chronic mucocutaneous candidiasis in humans with inborn errors of interleukin-17 immunity. *Science*. 2011;332(6025):65–68. doi:10.1126/science.1200439
32. Kuestner RE, Taft DW, Haran A, et al. Identification of the IL-17 receptor related molecule IL-17RC as the receptor for IL-17F. *J Immunol*. 2007;179(8):5462–5473. doi:10.4049/jimmunol.179.8.5462
33. Wright JF, Bennett F, Li B, et al. The human IL-17F/IL-17A heterodimeric cytokine signals through the IL-17RA/IL-17RC receptor complex. *J Immunol*. 2008;181(4):2799–2805. doi:10.4049/jimmunol.181.4.2799
34. Fossiez F, Djossou O, Chomarat P, et al. T cell interleukin-17 induces stromal cells to produce proinflammatory and hematopoietic cytokines. *J Exp Med*. 1996;183(6):2593–2603. doi:10.1084/jem.183.6.2593
35. Veldhoen M. Interleukin 17 is a chief orchestrator of immunity. *Nat Immunol*. 2017;18(6):612–621. doi:10.1038/ni.3742
36. Taniguchi K, Karin M. NF-κB, inflammation, immunity and cancer: coming of age. *Nat Rev Immunol*. 2018;18(5):309–324. doi:10.1038/nri.2017.142
37. Mitchell JP, Carmody RJ. NF-κB and the Transcriptional Control of Inflammation. *Int Rev Cell Mol Biol*. 2018;335:41–84. doi:10.1016/bs.ircmb.2017.07.007
38. Y-R X, Lei C-Q. TAK1-TABs complex: a central signalosome in inflammatory responses. *Front Immunol*. 2020;11:608976. doi:10.3389/fimmu.2020.608976
39. Amatya N, Garg AV, Gaffen SL. IL-17 signaling: the Yin and the Yang. *Trends Immunol*. 2017;38(5):310–322. doi:10.1016/j.it.2017.01.006
40. Liu K, Ding T, Fang L, et al. Organic selenium ameliorates -induced mastitis in rats by inhibiting the activation of NF-κB and MAPK signaling pathways. *Front Vet Sci*. 2020;7:443. doi:10.3389/fvets.2020.00443
41. Liu T, Zhang L, Joo D, Sun S-C. NF-κB signaling in inflammation. *Signal Transd Target Ther*. 2017;2(1). doi:10.1038/sigtrans.2017.23